

# Wood Adhesives

*Edited by*

A. Pizzi

K.L. Mittal

///VSP///



# Wood Adhesives

This page intentionally left blank

# Wood Adhesives

*Edited by*

A. Pizzi and K. L. Mittal

**///VSP///**

LEIDEN • BOSTON  
2010

CRC Press  
Taylor & Francis Group  
6000 Broken Sound Parkway NW, Suite 300  
Boca Raton, FL 33487-2742

© 2011 by Taylor & Francis Group, LLC  
CRC Press is an imprint of Taylor & Francis Group, an Informa business

No claim to original U.S. Government works  
Version Date: 20120525

International Standard Book Number-13: 978-9-00-419092-4 (eBook - PDF)

This book contains information obtained from authentic and highly regarded sources. Reasonable efforts have been made to publish reliable data and information, but the author and publisher cannot assume responsibility for the validity of all materials or the consequences of their use. The authors and publishers have attempted to trace the copyright holders of all material reproduced in this publication and apologize to copyright holders if permission to publish in this form has not been obtained. If any copyright material has not been acknowledged please write and let us know so we may rectify in any future reprint.

Except as permitted under U.S. Copyright Law, no part of this book may be reprinted, reproduced, transmitted, or utilized in any form by any electronic, mechanical, or other means, now known or hereafter invented, including photocopying, microfilming, and recording, or in any information storage or retrieval system, without written permission from the publishers.

For permission to photocopy or use material electronically from this work, please access [www.copyright.com](http://www.copyright.com) (<http://www.copyright.com/>) or contact the Copyright Clearance Center, Inc. (CCC), 222 Rosewood Drive, Danvers, MA 01923, 978-750-8400. CCC is a not-for-profit organization that provides licenses and registration for a variety of users. For organizations that have been granted a photocopy license by the CCC, a separate system of payment has been arranged.

**Trademark Notice:** Product or corporate names may be trademarks or registered trademarks, and are used only for identification and explanation without intent to infringe.

**Visit the Taylor & Francis Web site at**  
**<http://www.taylorandfrancis.com>**

**and the CRC Press Web site at**  
**<http://www.crcpress.com>**

# Contents

<b>Preface</b>	ix
<b>Part 1: Fundamental Adhesion Aspects in Wood Bonding</b>	
Natural Lignans as Adhesives for Cellulose: Computational Interaction Energy vs Experimental Results <i>M. Sedano-Mendoza, P. Lopez-Albarran and A. Pizzi</i>	3
Evaluation of Some Synthetic Oligolignols as Adhesives: A Molecular Docking Study <i>C. Martínez, M. Sedano, A. Munro, P. López and A. Pizzi</i>	21
Modification of Sugar Maple ( <i>Acer saccharum</i> ) and Black Spruce ( <i>Picea mariana</i> ) Wood Surfaces in a Dielectric Barrier Discharge (DBD) at Atmospheric Pressure <i>F. Busnel, V. Blanchard, J. Prégent, L. Stafford, B. Riedl, P. Blanchet and A. Sarkissian</i>	35
Determination of the Microstructure of an Adhesive-Bonded Medium Density Fiberboard (MDF) using 3-D Sub-micrometer Computer Tomography <i>G. Standfest, S. Kranzer, A. Petutschnigg and M. Dunky</i>	49
Influence of the Degree of Condensation on the Radial Penetration of Urea-Formaldehyde Adhesives into Silver Fir ( <i>Abies alba</i> , Mill.) Wood Tissue <i>I. Gavrilović-Grmuša, J. Miljković and M. Điporović-Momčilović</i>	63
Radial Penetration of Urea-Formaldehyde Adhesive Resins into Beech ( <i>Fagus Moesiaca</i> ) <i>I. Gavrilović-Grmuša, M. Dunky, J. Miljković and M. Djiporović-Momčilović</i>	81
A Flexible Adhesive Layer to Strengthen Glulam Beams <i>M. Brunner, M. Lehmann, S. Kraft, U. Fankhauser, K. Richter and J. Conzett</i>	97
Properties Enhancement of Oil Palm Plywood through Veneer Pretreatment with Low Molecular Weight Phenol-Formaldehyde Resin <i>Y. F. Loh, M. T. Paridah, Y. B. Hoong, E. S. Bakar, H. Hamdan and M. Anis</i>	135

- Reaction Mechanism of Hydroxymethylated Resorcinol Adhesion Promoter in Polyurethane Adhesives for Wood Bonding  
*A. Szczurek, A. Pizzi, L. Delmotte and A. Celzard* 145

## Part 2: Synthetic Adhesives

- Optimization of the Synthesis of Urea-Formaldehyde Resins using Response Surface Methodology  
*J. M. Ferra, P. C. Mena, J. Martins, A. M. Mendes, M. R. N. Costa, F. D. Magalhães and L. H. Carvalho* 153
- Characterization of Urea-Formaldehyde Resins by GPC/SEC and HPLC Techniques: Effect of Ageing  
*J. M. Ferra, A. M. Mendes, M. R. N. Costa, F. D. Magalhães and L. H. Carvalho* 171
- Formaldehyde-Free Dimethoxyethanal-Derived Resins for Wood-Based Panels  
*M. Properzi, S. Wieland, F. Pichelin, A. Pizzi and A. Despres* 189
- Melamine-Formaldehyde Resins without Urea for Wood Panels  
*E. Pendlebury, H. Lei, M.-L. Antoine and A. Pizzi* 203
- Bonding of Heat-Treated Spruce with Phenol-Formaldehyde Adhesive  
*M. Kariz and M. Sernek* 211
- Influence of Nanoclay on Phenol-Formaldehyde and Phenol-Urea-Formaldehyde Resins for Wood Adhesives  
*H. Lei, G. Du, A. Pizzi, A. Celzard and Q. Fang* 225
- Emulsion Polymer Isocyanates as Wood Adhesive: A Review  
*K. Grøstad and A. Pedersen* 235
- Adhesives for On-Site Rehabilitation of Timber Structures  
*H. Cruz and J. Custódio* 261

## Part 3: Environment-Friendly Adhesives

- Thermal Characterization of Kraft Lignin Phenol-Formaldehyde Resin for Paper Impregnation  
*A. R. Mahendran, G. Wuzella and A. Kandelbauer* 291
- Acacia mangium* Tannin as Formaldehyde Scavenger for Low Molecular Weight Phenol-Formaldehyde Resin in Bonding Tropical Plywood  
*Y. B. Hoong, M. T. Paridah, Y. F. Loh, M. P. Koh, C. A. Luqman and A. Zaidon* 305
- Synthesis of Modified Poly(vinyl acetate) Adhesives  
*A. Salvini, L. M. Saija, M. Lugli, G. Cipriani and C. Giannelli* 317

Acrylated Epoxidized Soy Oil as an Alternative to Urea-Formaldehyde in Making Wheat Straw Particleboards <i>M. Tasooji, T. Tabarsa, A. Khazaeian and R. P. Wool</i>	341
Gluten Protein Adhesives for Wood Panels <i>H. Lei, A. Pizzi, P. Navarrete, S. Rigolet, A. Redl and A. Wagner</i>	353
Wood Panel Adhesives from Low Molecular Mass Lignin and Tannin without Synthetic Resins <i>P. Navarrete, H. R. Mansouri, A. Pizzi, S. Tapin-Lingua, B. Benjelloun-Mlayah, H. Pasch and S. Rigolet</i>	367
<b>Part 4: Wood Welding and General Paper</b>	
Wood-Dowel Bonding by High-Speed Rotation Welding — Application to Two Canadian Hardwood Species <i>G. Rodriguez, P. Diouf, P. Blanchet and T. Stevanovic</i>	383
Chemical Changes Induced by High-Speed Rotation Welding of Wood — Application to Two Canadian Hardwood Species <i>Y. Sun, M. Royer, P. N. Diouf and T. Stevanovic</i>	397
Moisture Sensitivity of Scots Pine Joints Produced by Linear Frictional Welding <i>M. Vaziri, O. Lindgren, A. Pizzi and H. R. Mansouri</i>	415
High Density Panels Obtained by Welding of Wood Veneers without any Adhesives <i>H. R. Mansouri, J.-M. Leban and A. Pizzi</i>	429
Overview of European Standards for Adhesives Used in Wood-Based Products <i>F. Simon and G. Legrand</i>	435

This page intentionally left blank

## Preface

Wood adhesives are of tremendous industrial importance as more than two-thirds of wood products today in the world are totally, or at least partially, bonded together using a variety of adhesives. The reason being that adhesive bonding offers many advantages *vis-à-vis* other joining methods for wood components.

Even a cursory look at the literature will evince that currently there is brisk R&D activity in devising new wood adhesives or ameliorating the existing ones. The modern mantra in all industrial sectors is: 'Think green, go green' and the wood industry is no exception. This new refrain has spurred much research activity in synthesizing environmentally-benign and human-friendly wood adhesives. One specific example is the elimination of formaldehyde emissions from wood adhesives and many alternate avenues have been explored in this vein.

Considering the industrial and commercial importance of wood adhesives and the high tempo of research in understanding and improving adhesion strength of wood adhesives we decided to bring out this special volume which reflects the collective wisdom of a contingent of world-class researchers in this technologically highly important field.

This book is based on the Special Issue of the *Journal of Adhesion Science and Technology (JAST)* which was published as Vol. 24, Nos 8–10 (2010). Based on the widespread interest and tremendous importance of wood adhesives in construction and other industries, we decided to bring out this book as a single and easily available source of information. The papers as published in the above-mentioned Special Issue have been rearranged in a more logical fashion in this book.

This book contains a total of 28 papers (reflecting overviews and original research) covering many ramifications of wood adhesives and is divided into four parts as follows: Part 1: Fundamental Adhesion Aspects in Wood Bonding; Part 2: Synthetic Adhesives; Part 3: Environment-Friendly Adhesives; and Part 4: Wood Welding and General Paper. The topics covered include: computation of interfacial interactions between resin oligomers and cellulose substrates by theoretical molecular mechanics means; treatment of wood surfaces by atmospheric pressure plasma; application of computer tomography in determination of microstructures in bonded fiberboards; penetration of adhesives in wood species; veneer pretreat-

ment; strengthening of glulam beams; resorcinol adhesion promoter; synthesis and characterization of a variety of adhesives for wood bonding; influence of fillers (e.g., nanoclay) on resins for wood bonding; adhesives for on-site rehabilitation of timber structures; development of adhesives to eliminate or reduce formaldehyde emission; gluten protein adhesives for wood panels; lignin- and tannin-based adhesives; wood welding; wood connections without use of adhesives; and overview of European standards for adhesives used in wood-based products.

We sincerely hope this book containing bountiful up-to-date information, including some novel approaches to wood bonding/wood connections, will be of great value to anyone interested in this highly industrially important topic. This book should serve as repository of information and a commentary on current R&D activity dealing with wood adhesives. We further hope this book will serve as a fountainhead for new research ideas to further enhance the performance and durability of wood-based products.

### *Acknowledgements*

Now it is our great pleasure to thank all those who made this book possible. First and foremost our thanks are extended to the authors for their interest, enthusiasm, cooperation and contribution without which this book could not be materialized. We profusely thank the unsung heroes (reviewers) for their time and efforts in providing many valuable comments as comments from peers are *sine qua non* to maintain the highest standard of publication. We would be remiss if we do not extend our appreciation to the appropriate individuals at Brill (publisher) for giving this book a body form.

A. PIZZI  
ENSTIB-LERMAB  
University Henri Poincare — Nancy 1  
BP 1041  
88051 Epinal cedex 9, France  
E-mail: antonio.pizzi@enstib.uhp-nancy.fr

K. L. MITTAL  
P.O. Box 1280  
Hopewell Jct., NY 12533, USA

**Part 1**  
**Fundamental Adhesion Aspects in**  
**Wood Bonding**

This page intentionally left blank

# Natural Lignans as Adhesives for Cellulose: Computational Interaction Energy vs Experimental Results

M. Sedano-Mendoza<sup>a,b</sup>, P. Lopez-Albarran<sup>b,\*</sup> and A. Pizzi<sup>a</sup>

<sup>a</sup> ENSTIB-LERMAB, Nancy University, University Henri Poincaré, 27 rue du Merle Blanc, BP 1041, 88051 Epinal, France

<sup>b</sup> Facultad de Ingenieria en Tecnologia de la Madera, Universidad Michoacana de San Nicols de Hidalgo, Campus Morelia, Av. Fco. J. Muciga S/N, CP: 58030, Morelia, Michoacan, Mexico

---

## Abstract

Comparison between the molecular mechanics calculated energy of interaction of lignan dimers and trimers with a cellulose I crystallite and the experimental values of Young's modulus obtained by thermomechanical analysis (TMA) of cellulose paper impregnated with low molecular weight lignins showed good correlation between calculated and experimental results. The oligomer composition of the four low molecular weight lignins tested was obtained by MALDI-TOF mass spectrometry. This showed that these lignins were predominantly composed of dimers and trimers rendering them ideal for correlation testing. The lignan/cellulose crystallite interaction energy is determined by the oligomer molecular weight as well as the type of linkage within the lignan oligomers. Lignans with higher molecular weight in which the units are linked as  $\beta$ -O-4 give interaction energy values indicating stronger attraction with cellulose.

## Keywords

Adhesives, molecular mechanics, lignans, lignins, thermomechanical analysis, interaction energy, cellulose

## 1. Introduction

Lignin is the second most abundant renewable biopolymer in the world, exceeded in quantity only by cellulose, comprising 30% of all non-fossil organic carbon [1] and constituting from a quarter to a third of the dry mass of wood. Its precursors are three monolignol monomers, methoxylated to various degrees by enzymatic reaction *via* a free radical route: *p*-coumaryl alcohol, coniferyl alcohol, and sinapyl alcohol [2].

The amounts and types of monolignols produced or present in lignin depend on the treatment that the raw lignin has undergone. Guaiacyl units are usually more abundant in softwood than hardwood, the latter one presenting a similar proportion of guaiacyl and syringyl units. Lignin in solution has a composition which differs

---

\* To whom correspondence should be addressed. E-mail: plopez@umich.mx

from protolignin (native lignin as present in wood before extraction) due to the extraction process used. However, in general, the most abundant linkages between lignin units are the  $\beta$ -O-4,  $\beta$ 5 and  $\beta\beta$  [3].

The need to substitute synthetic thermosetting wood adhesives with more environmentally acceptable resins has led to intense research on adhesives derived from natural, non-toxic materials. Extensive reviews on the subject exist [4, 5]. It is sufficient here to state that lignin is one of the materials at the forefront of these studies. Numerous wood adhesive formulations based on lignin have been published over the years [6].

In the study presented in this article several types of industrial lignins have been investigated: (a) a low molecular weight organosolv grass lignin from India, (b) an organosolv lignin from miscanthus grass, (c) a kraft lignin depolymerized according to a published procedure, and (d) a depolymerized form of the lignin in (a) above. The molecular mechanics adhesion calculations of all the secondary forces interactions with crystalline cellulose have been limited so far to the short oligomers found to compose these lignins.

To determine the main dimers and trimers in such lignins, MALDI-TOF (matrix assisted laser desorption ionisation time-of-flight) mass spectrometry was used. In principle MALDI-TOF is matrix-assisted, thus, the sample under test is dried together with a light absorbing compound (matrix). A pulse of laser light is used to force molecules into gas phase and ionize them. The ions are then accelerated in an electrical field. They are then allowed to drift in the mass spectrometer and are picked up by a detector. The drift time is measured electronically. The drift time thus measured allows determination of the molecular weight because drift time is proportional to velocity and the acceleration is proportional to mass. Calibration is done by simultaneous analysis of standards of known masses. The result is a mass spectrum where the peaks indicate clearly the oligomers present.

However, fundamental molecular mechanics studies on the interaction of the lower molecular weight oligomers of lignin with cellulose have been carried out but without checking if the values obtained corresponded or could be correlated to Young's modulus values obtained experimentally. Such an approach has already proven its worth in the correlation found between adhesive/substrate interactions calculated by molecular mechanics and experimental bond strength obtained for phenol-formaldehyde and urea-formaldehyde thermosetting adhesives to cellulose [7–10]. The same approach but using considerably more modern molecular mechanics algorithm has been adopted in this article for the interaction of short lignin oligomers with cellulose.

## 2. Experimental

The types of lignins used were: (a) an industrial organosolv grass lignin (Ln\_India) Protobind 100SA.140 India Lignin, provided by Granit<sup>®</sup>, Switzerland [11]; (b) a laboratory organosolv lignin from miscanthus (*Miscanthus giganteus*) grass

(Ln\_miscanthus) [12]; (c) a depolymerized kraft lignin (Ln\_CO2) Ln-T-CO2-1 [13], and (d) (Ln\_India\_depo) depolymerised Indian lignin from sample (a) [14].

AutoDock [15] is a tool for molecular modelling that provides a procedure for predicting the interaction of small molecules with macromolecular targets. The ideal procedure would find the global minimum in the interaction energy between the substrate and the target molecule, exploring all available degrees of freedom for the system. In order to represent our specific interest the ligand is represented by the lignan (oligolignols) target and the substrate by crystalline cellulose. AutoDock has a free energy scoring function that is based on a linear regression analysis, the AMBER [16] force field.

The MALDI-TOF spectra were recorded on a KRATOS Kompact MALDI AX-IMA TOF 2 instrument. The irradiation source was a pulsed nitrogen laser with a wavelength of 337 nm. The length of one laser pulse was 3 ns. The measurements were carried out using the following conditions: polarity-positive, flight path-linear, mass-high (20 kV acceleration voltage), and 100–150 pulses per spectrum. The delayed extraction technique was used by applying delay times of 200–800 ns.

The samples were prepared by mixing the lignin water solutions with acetone (4 mg/ml, 50/50 water/acetone by volume). The sample solutions so prepared were mixed with an acetone solution of the matrix (10 mg matrix solution per ml acetone). As the matrix 2,5-dihydroxy benzoic acid was used. For enhancement of ion formation, NaCl was added to the matrix (10 mg/ml in water). The solutions of the sample and the matrix were mixed in proportions 3 parts matrix solution + 3 parts lignin solution + 1 part NaCl solution, and 0.5 to 1  $\mu$ l of the resulting solution mix were placed on the MALDI target. After evaporation of the solvent the MALDI target was introduced into the spectrometer. The dry droplet sample preparation method was used.

Commercial  $\alpha$ -cellulose sheets (14.5 mm  $\times$  5.5 mm  $\times$  0.17 mm) were used as sample with 89.62 g/m<sup>2</sup> of lignin, hexamine hardener (5% on lignan grammage) and with 1.53% paper moisture content. The lignins were dissolved at 42% solids content at pH 12. The paper samples were then impregnated, and dried in an oven at 36°C.

TMA tests were carried out on the dried, lignin impregnated papers. Tensile tests on the dry specimens were conducted on a Mettler 40 TMA apparatus. The specimen was subjected to an oscillating force. The Young's modulus was obtained as a function of temperature by applying the formula:

$$E = \Delta FL_0 / (A\Delta L), \quad (1)$$

where:

$E$ : Young's modulus of lignin impregnated paper sheet (N/mm<sup>2</sup>),

$\Delta F$ : difference between maximum and minimum values of the oscillating force applied (N),

$L_0$ : sample length (mm),

A: sample area (thickness) (width) ( $\text{mm}^2$ ),

$\Delta L$ : length change (mm).

The weight percentage of each oligomer in the MALDI-TOF spectrum of each lignin was determined. These weight percentages were multiplied by the maximum value of Young's modulus obtained by TMA for the lignin sample being tested and thus an approximation of the contribution of each oligomer to the strength of the lignin/cellulose composite was determined.

The theoretical molecular mechanics calculation of the highest energy of interaction of individual oligolignans dimers and trimers with model cellulose I crystallite composed of three layers each of 6 by 12 glucose residues has been carried out with AutoDock Version 4.2 [17, 18]. Visualization of the minimum energy conformation for the interaction is made with MOLDEN 3.9 [19], gOpenMol 2.32 [20, 21] and Molekel 4.3 [22, 23] for Linux computer operating system. AutoDock calculations are performed in several steps: (1) preparation of the coordinates files of a model substrate and of the lignan including its hydrogen atoms, atomic partial charges and atoms types, and also information on the torsional degrees of freedom; (2) recalculation of atomic affinities, which is a rapid energy evaluation that is achieved by calculating atomic affinity potential for each atom type in the lignan, and (3) Docking simulation carried out using a semi-empirical free energy force field to evaluate conformations during docking simulations (Fig. 1).

The force field calculates the interaction energies in two steps. The lignan and the substrate start in an unbound conformation. In the first step, the intermolecular energetics is estimated for the transition from this unbound state to the conformation of the lignan and substrate in the bound state. The second step then evaluates the intermolecular energetics of combining the lignan and the substrate in their bound conformation.

The force field includes six pair-wise evaluations ( $V$ ) and estimate of the conformational entropy lost upon binding ( $\Delta S_{\text{conf}}$ ):

$$\Delta G = (V_{\text{bound}}^{\text{L-L}} - V_{\text{unbound}}^{\text{L-L}}) + (V_{\text{bound}}^{\text{P-P}} - V_{\text{unbound}}^{\text{P-P}}) + (V_{\text{bound}}^{\text{P-L}} - V_{\text{unbound}}^{\text{P-L}} + \Delta S_{\text{conf}}), \quad (2)$$

where  $L$  refers to the "lignan" and  $P$  refers to the "substrate" in a lignan–substrate docking calculation. Each interaction includes evaluations for dispersion/repulsion van der Waals (vdW), hydrogen bonding (hbond), electrostatic (elec), and desolvation (sol) energies between a pair of atoms  $i$  and  $j$ :

$$V = W_{\text{vdW}} \sum_{i,j} [(A_{ij}/r_{ij}^{12}) - (B_{ij}/r_{ij}^6)] + W_{\text{hbond}} \sum_{i,j} E(t)[(C_{ij}/r_{ij}^{12}) - (D_{ij}/r_{ij}^{10})] + W_{\text{elec}} \sum_{i,j} [q_i q_j / \varepsilon(r_{ij}) r_{ij}] + W_{\text{sol}} \sum_{ij} (S_i V_j + S_j V_i) e^{(-r_{ij}^2/2\sigma^2)}, \quad (3)$$

where  $q_i$  and  $q_j$  are, respectively, the electrostatic charges of atoms  $i$  and  $j$ ;  $r_{ij}$  is the distance between atoms  $i$  and  $j$ .

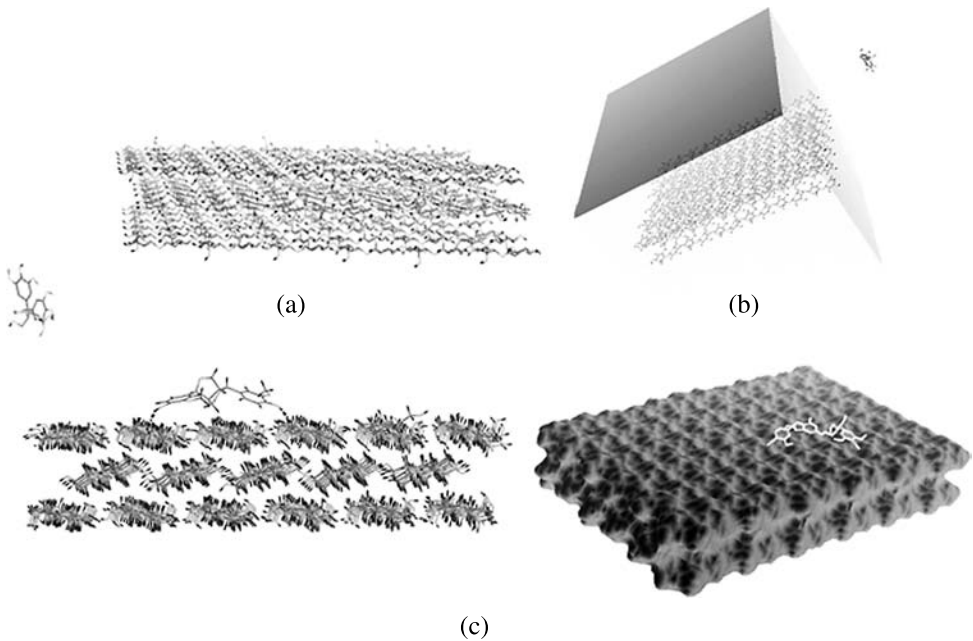


**Figure 1.** Examples of molecular mechanics interactive docking of a lignan trimer on a cellulose I crystallite. (a) and (b) different positions of the oligomer in relation to the cellulose crystallite at the start of the docking simulation, as the oligomer progressively approaches the cellulose crystallite. (c) Different views of the position, conformation and site of minimum energy of the lignan/cellulose system.

The weighting constants  $W$  have been optimized to standardize the empirical free energy based on a set of experimentally-determined binding constants. The first term is a typical 6/12 potential function of the Lennard–Jones type [24, 25] for dispersion/repulsion interactions. The parameters are based on the Amber force field. The second term is a directional H-bond term based on a 10/12 potential function. The parameters  $C$  and  $D$  are assigned to give a maximum energy well depth of 5 kcal/mol at a 1.9 Å distance for hydrogen bonds between oxygen and nitrogen ( $C$ ), and an energy well depth of 1 kcal/mol ( $D$ ). The function  $E(t)$  provides directionality based on the angle  $t$  from the ideal H-bonding geometry. The third term is a screened Coulomb potential for electrostatic non-directional interactions. The final term is a desolvation potential based on the volume of atoms ( $V$ ) that surround a given atom and shelter it from the solvent, weighted by solvation parameter ( $S$ ) and an exponential term with distance weighting factor  $\sigma = 3.5$  Å [26, 27].

It must be clearly pointed out that in molecular mechanics, by convention, an energy with a negative sign indicates that two molecules attract each other, hence, their interaction is attractive. A positive sign energy value indicates instead that the two molecules repel each other. Thus, the more negative is the energy of interaction, the more strongly attracted to each other are the two molecules.

### 3. Results and Discussion

In Fig. 1 is shown the example of a lignan trimer docking onto the surface of a cellulose crystallite. Fig. 1(a) and (b) show the initial positions at which the lignan is placed in relation to the cellulose crystallite, at a distance where interaction between the two is too small to be of any significance. As the lignan approaches the surface its conformation changes to adapt itself to the surface of the cellulose crystallite to minimize the total energy of the system until the lignan conformation of minimum energy is reached (Fig. 1(c)). In Fig. 1(c) the position of the trimer in relation to the section of the cellulose crystallite is shown.

The experimental TMA tensile test results in Table 1 show that the interaction with cellulose of the (Ln\_India) lignin yields a Young's modulus higher than that of the three other lignins used independently of solids content of the impregnating lignin solution as shown from the higher Young's modulus obtained. Fig. 2 shows the elongation curves as a function of temperature obtained in the TMA tensile test that have allowed to calculate the modulus values in Table 1. MALDI TOF analysis of the four lignins tested indicated that these were very low molecular weight lignins composed almost exclusively of dimers and trimers. The MALDI-TOF spectra of these 4 lignins are shown in Figs 3–6 for the interval 200–750 Da. The MALDI-TOF spectra between 60 and 200 Da were recorded but are not re-

**Table 1.**

Results of: (1) Young's modulus of cellulose paper sheets impregnated with solutions of different lignins (Ln-CO<sub>2</sub>; Ln-depol; Ln-miscanthus; Ln-India) at different lignin solids concentrations of the impregnating aqueous solution (42%, 22%, 15%, 11%), and (2) the percentage modulus increase over non-impregnated paper control

Non-impregnated control		Young's modulus (MPa)	Young's modulus increase (%)
		0.80	–
42% solids	Ln_CO2	2.01	151
	Ln_depol	2.63	228
	Ln-miscanthus	3.33	317
	<b>Ln_India</b>	<b>4.50</b>	<b>463</b>
22% solids	Ln_CO2	1.22	53
	Ln_depol	1.71	114
	Ln-miscanthus	1.84	130
	<b>Ln_India</b>	<b>3.80</b>	<b>375</b>
15% solids	Ln_CO2	1.76	120
	Ln_depol	1.84	129
	Ln-miscanthus	1.92	140
	<b>Ln_India</b>	<b>2.60</b>	<b>225</b>
11% solids	Ln_CO2	1.00	25
	Ln_depol	1.48	85
	Ln-miscanthus	1.73	117
	<b>Ln_India</b>	<b>2.48</b>	<b>210</b>

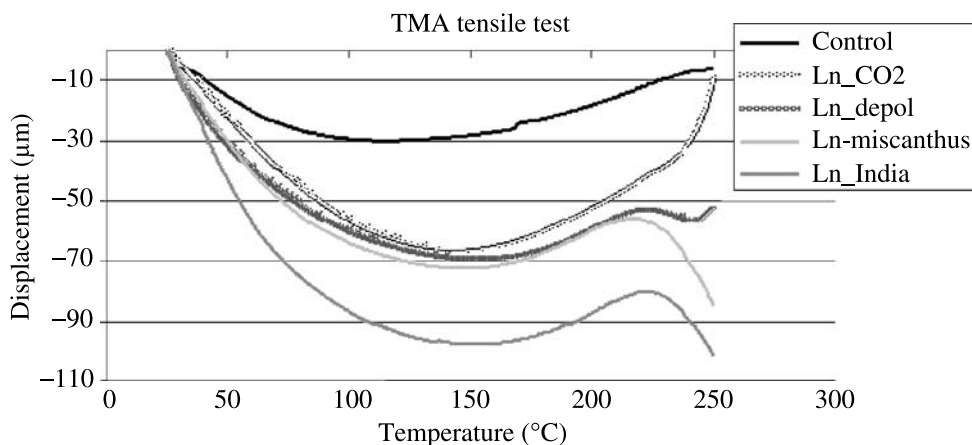


**Figure 2.** Thermomechanical analysis of tensile test on paper impregnated with different types of low molecular weight lignins: displacement as a function temperature. Standard is the displacement obtained with non-impregnated paper used as a control.

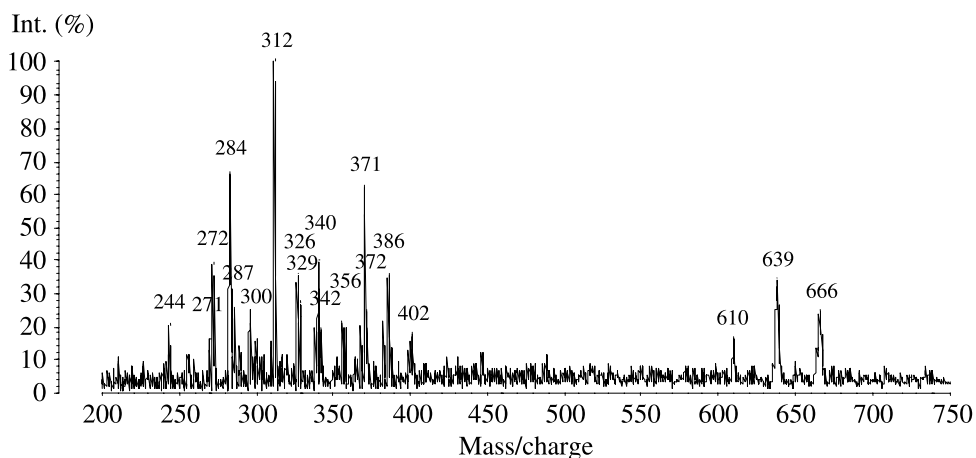


**Figure 3.** MALDI-TOF spectrum of original lignin Ln\_India.

ported here. However, the relevant assignment of the MALDI-TOF peaks and their distribution are reported in Tables 2 and 3. In Table 2 are shown all the relevant peaks in the spectra in Figs 3–6 with the calculated molecular mass + 23 Da (for the  $\text{Na}^+$  matrix) for the relevant corresponding oligomers and their relative intensity expressed as a percentage of the highest peak.

To explain the shortened nomenclature used in Table 2, lignin units are of the H-type, guayacil-type (G-type) and syringyl-type (GS-type) [28]. As examples, for Lignin Ln\_CO<sub>2</sub> the peaks at 113 and 181 indicate that H<sub>FRACTION</sub> and GS<sub>FRACTION</sub> correspond to fragments, respectively, of H-type and GS-type monomers the calculated peak values of which are given by the molecular weight of the oligomer

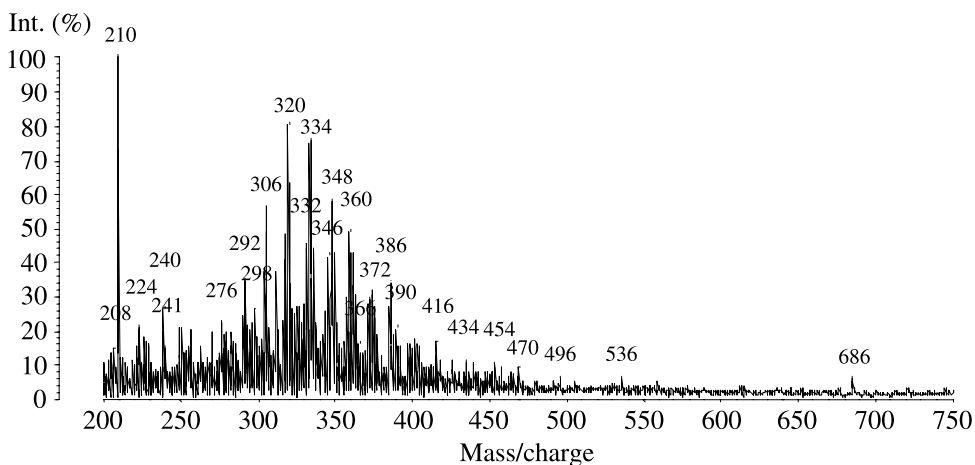


Figure 4. MALDI-TOF spectrum of lignin Ln\_India depolymerized.

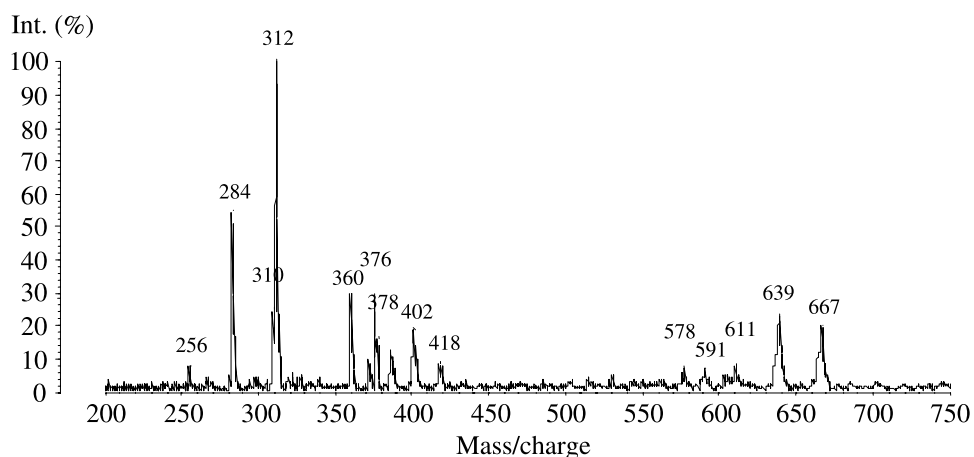
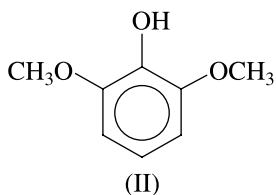
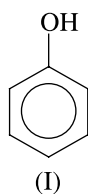
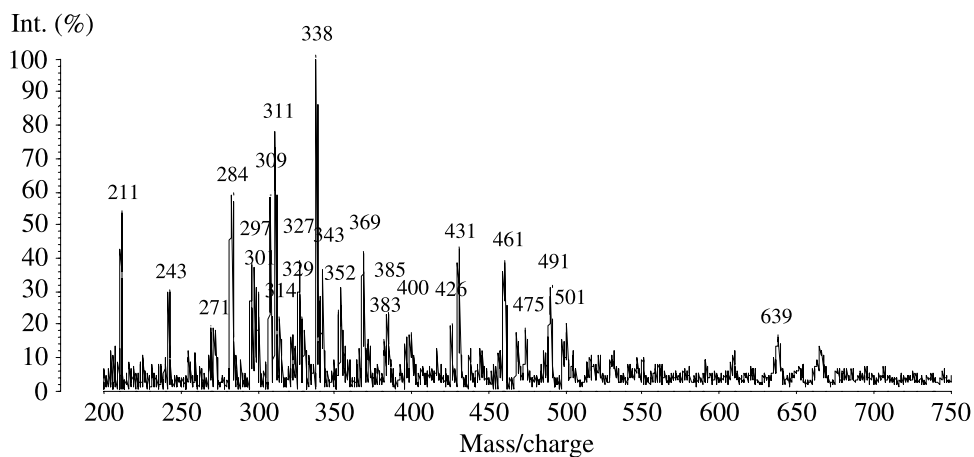


Figure 5. MALDI-TOF spectrum of lignin Ln\_CO<sub>2</sub>.

plus that of the Na matrix, thus peaks at  $93 + 23(\text{Na}^+)$  Da = 116 Da (117 Da is protonated) and  $154 + 23(\text{Na}^+)$  Da = 177 Da are obtained. These correspond to structures (I) and (II), respectively.





**Figure 6.** MALDI-TOF spectrum of depolymerized miscanthus lignin, Ln\_miscanthus.

**Table 2.**

Interpretation of MALDI TOF peaks in Figs 3–6

Dimer/trimer	Molecular weight +Na	Peak (Da)	Relative peak height* (%)	Young's modulus related to relative peak height (MPa)
Lignin Ln_CO2-1				
H <sub>FRACTION</sub>	117	113	65	1.03
GS <sub>FRACTION</sub>	177	181	40	0.84
H + GS	383	378	30.5	0.61
G + GS <sub>FRACTION</sub>	356	360	30	0.6
GS + G <sub>FRACTION</sub>				
G + G + GS	593	591	8	0.16
H + GS + GS				
Lignin miscanthus				
H <sub>FRACTION</sub>	117	121	18	0.6
G <sub>FRACTION</sub>	147	147	25	0.83
GS <sub>FRACTION</sub>	177	177	18	0.6
G	203	198	10.5	0.35
H + H <sub>FRACTION</sub>	266	271	20	0.66
H + G <sub>FRACTION</sub>	296	297	38	1.26
G + H <sub>FRACTION</sub>				
GS (-CH <sub>3</sub> ) + H <sub>FRACTION</sub>	337	338	100	
H + H	323	322	17	0.56
H + GS <sub>FRACTION</sub>	326	327	38	1.26
G + G <sub>FRACTION</sub>				
GS + H <sub>FRACTION</sub>				
G + GS <sub>FRACTION</sub>	356	352	24.5	0.82

**Table 2.**

(Continued.)

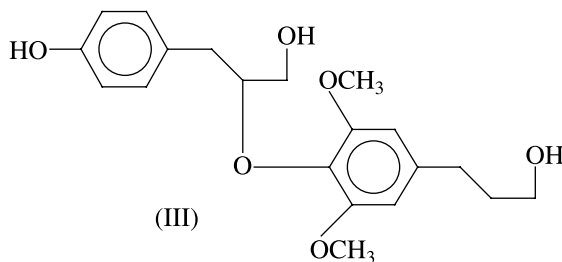
Dimer/trimer	Molecular weight +Na	Peak (Da)	Relative peak height* (%)	Young's modulus related to relative peak height (MPa)
GS + GFRACTION				
G + GS <sub>FRACTION</sub>	356	355	32	1.07
GS + GFRACTION				
H + GS	383	383	15.5	0.52
G + G				
GS + GS <sub>FRACTION</sub>	386	385	23.6	0.79
H + H + H	473	475	19	0.82
G + G + H <sub>FRACTION</sub>	477			
H + H + G	503	501	21	0.7
Lignin India depolymerized				
H <sub>FRACTION</sub>	117	117	13	0.34
G <sub>FRACTION</sub>	147	149	32	0.84
GS <sub>FRACTION</sub>	177	177	23	0.61
G	203	208	16	0.42
G + H <sub>FRACTION</sub>	296	298	38	0.1
H + H	323	322	43.2	1.14
H + GS <sub>FRACTION</sub>	326	326	34.7	0.91
G + GS <sub>FRACTION</sub>	356	352	20.5	0.54
GS + GFRACTION				
G + GS <sub>FRACTION</sub>	357	360	52	1.37
GS + GFRACTION				
GS + GS <sub>FRACTION</sub>	387	386	36	0.95
G + GS	413	416	18	0.47
H + H + H <sub>FRACTION</sub>	417			
H + H + H	473	470	10	0.26
G + GS + G <sub>FRACTION</sub>	537	536	7	0.18
GS + GS + H <sub>FRACTION</sub>				
H + GS + GS				
Lignin India original				
G + H <sub>FRACTION</sub>	297	300	17.3	0.78
H + GS <sub>FRACTION</sub>	327	326	38.2	1.72
G + G <sub>FRACTION</sub>				
GS + H <sub>FRACTION</sub>				
G + GS <sub>FRACTION</sub>	356	356	22.7	1.02
GS + GFRACTION				
GS + GS <sub>FRACTION</sub>	386	386	37.3	1.70

Equally, as an example, the dimer H + GS at an actual peak 385 Da corresponds to an oligomer of molecular weight 360 this plus the 23 Da of the Na<sup>+</sup> gives 360 + 23(Na<sup>+</sup>) Da = 383 Da (structure III)

**Table 3.**

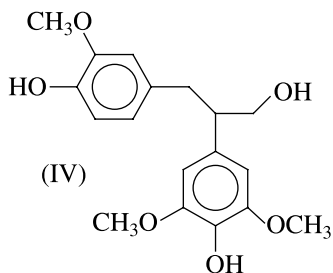
MALDI-TOF peaks with specific links to lignan oligomers of which the interaction energy with cellulose has been calculated

Dimer/trimer	Molecular weight +Na	Peak (Da)	Relative peak height* (%)	Young's modulus related to relative peak height (MPa)
Lignin Ln_CO2				
G_γβ_G	383	378	16	0.32
G_βO4_G	399	402	20	0.40
G_αO4_G				
G_αβ_G	417	418	10	0.20
G_βO4_G_ββ_G	577.6	578	7.7	0.16
G_βO4_G_β5_G				
G_β5_G_γβ_GS	591.6	591	7.7	0.16
G_βO4_G_ββ_GS	607.6	611	8.8	0.18
G_βO4_GS_β5_G				
G_βO4_GS_ββ_GS	637.6	639	24.4	0.49
GS_βO4_GS_ββ_GS	667.6	667	20	0.40
Lignin miscanthus				
G_γβ_G	383	383	14.5	0.48
G_βO4_G	399	400	17.3	0.58
G_αO4_G				
G_βO4_GS	429.4	431	43.6	1.45
GS_βO4_GS	459.4	461	39.1	1.3
GS_αO4_GS				
GS_αβ_GS	477.5	475	18.2	0.61
G_βO4_GS_ββ_GS	637.6	639	16.4	0.55
Lignin India depolymerized				
G_γβ_G	383	386	36	0.95
G_αβ_G	417	416	18	0.47
G_βO4_G	429.4	434	12	0.32
GS_βO4_GS	459.4	454	10	0.26
GS_αO4_GS				



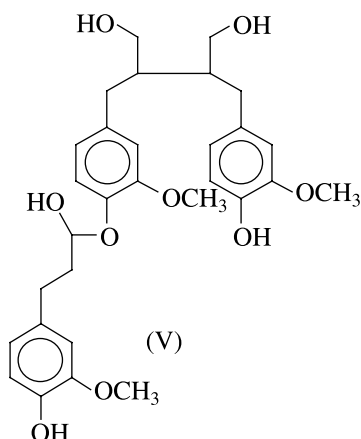
Where the H- and GS-type units can either be linked with the most common β-O-4 linkage or with other linkages which are allowed between lignin units [28]. Equally the peak at 360 Da corresponds to a dimer G + GS<sub>FRACTION</sub> the calculated

molecular weight of which is 337, thus giving  $337 + 23(\text{Na}^+) \text{ Da} = 360 \text{ Da}$  which corresponds to structure (IV)



Thus, while it is quite possible to identify which compounds are dimers and which are trimers, fragments or monomers, and which lignin units are involved, it is not strictly possible to define which types of linkages tie the units together, although these types are relatively few in lignin.

Table 3 shows the dimers and trimers that could be exactly identified in the MALDI-TOF spectra and for which the minimized interaction energies between the oligomer and the cellulose surface were calculated exactly. For each oligomer the calculated and experimental molecular weight + 23 ( $\text{Na}^+$ ) Da peaks are shown, as well as their interaction energy calculated by molecular mechanics and their percentages relative to the highest peak. From these the percentage by weight of each oligomer in the sample can be calculated. To explain the nomenclature used again for Lignin  $\text{Ln\_CO}_2$ ,  $\text{G\_}\beta\text{O}_4\text{G}$  indicates a dimer composed of two guayacil units linked by a  $\beta\text{-O-4}$  linkage [28]. For example, in the  $\text{G\_}\beta\text{O}_4\text{G\_}\beta\beta\text{G}$  trimer two of the guayacil units are linked by a  $\beta\text{-O-4}$  linkage and the third is linked to one of the other two by  $\beta\beta$  linkage corresponding to structure (V).



As only lignins of low molecular weight are studied, dimers and trimers have exclusively been found in the composition of the four lignins studied. However, it is not necessary to calculate the theoretical interaction energy with cellulose for

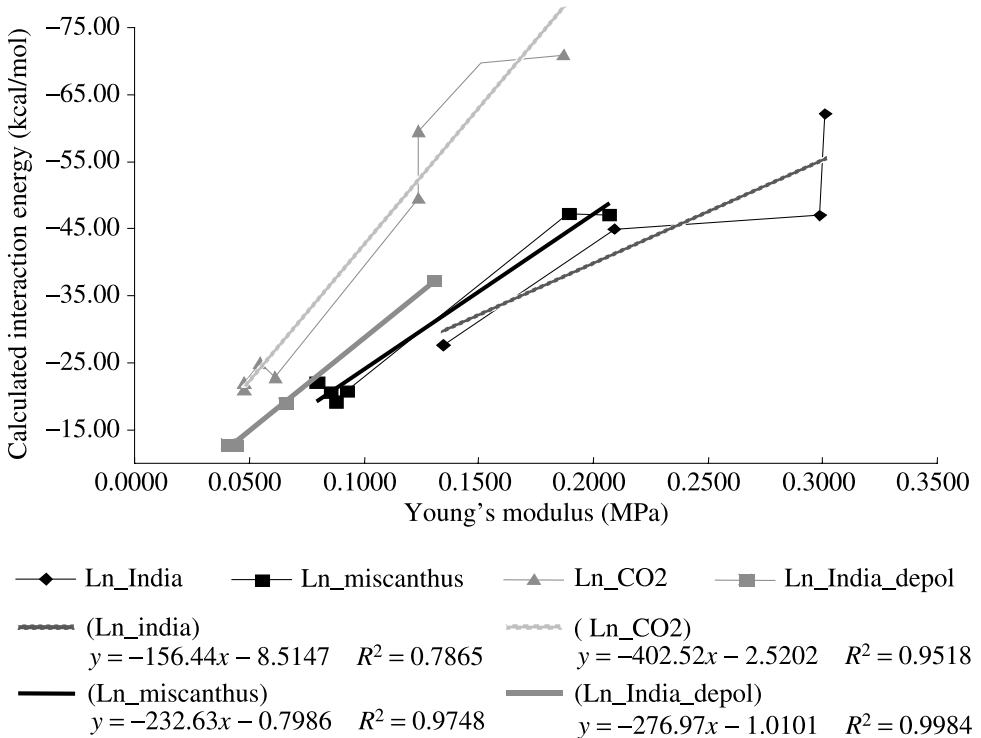


**Figure 7.** Correlation of experimental Young's modulus and molecular mechanics calculated (kcal/mol) interaction energies for low molecular weight lignins with cellulose.

all the dimers that are shown to exist in different percentages in the MALDI-TOF spectra. The results in Table 6 and in Fig. 7 indicate that if the calculation of the energy of interaction with the substrate of 20% or more by mass of the dimers and trimers is taken into account the trends correspond well to the Young's modulus obtained experimentally. That this is the case is evident from the results of the non-depolymerized (Ln\_India) where the interaction with the substrate of only 10% of the weight of the oligomers present in the mix could be calculated. In this case the coefficient of correlation (Fig. 7) is poor. This is shown in Table 4 presenting, for the different oligomers considered, predicted energies of interaction obtained by molecular mechanics calculation and experimental Young's modulus values obtained by TMA (Table 4). The Young's modulus values obtained by TMA have already been shown to correlate with interaction energies obtained by molecular mechanics [29, 30]. In order to compare the two parameters Fig. 7 is presented. It shows that the trend in Young's modulus for each lignan is maintained for both calculated energy and Young's modulus. The correlation coefficients  $R^2$  between the experimental values for the interaction energy with cellulose represented by Young's modulus and the theoretically calculated values for the different lignans are excellent at 0.95, 0.97 and 0.998 for (Ln\_CO2), (Ln\_miscanthus) and (Ln\_India\_depol), respectively.

**Table 4.**

Calculated interaction energy of lignan components with crystalline cellulose

Dimer/trimer	Composition (%)	ADT 42 (kcal/mol) per lignan	ADT 42 (kcal/mol) per lignin mix type	Young's modulus (MPa)
<b>Ln_India</b>				
G_βO4_GS_ββ_GS	6.69	−9.28	−62.08	0.3011
G_ββ_G	6.64	−7.08	−47.01	0.2988
GS_βO4_GS_ββ_GS	4.65	−9.67	−44.97	0.2093
G_βO4_GS_β5_G	2.99	−9.24	−27.63	0.1346
<b>TOTAL</b>	<b>20.97</b>	<b>−35.27</b>	<b>−181.69</b>	<b>0.9437</b>
<b>Ln_miscanthus</b>				
G_βO4_GS	6.21	−7.58	−47.07	0.2068
GS_βO4_GS	5.68	−8.32	−47.26	0.1891
G_γβ_G	2.77	−7.50	−20.78	0.0922
GS_αβ_GS	2.64	−7.30	−19.27	0.0879
G_βO4_G	2.57	−8.05	−20.69	0.0856
G_βO4_GS_ββ_GS	2.38	−9.28	−22.09	0.0793
<b>TOTAL</b>	<b>22.25</b>	<b>−48.03</b>	<b>−177.15</b>	<b>0.7409</b>
<b>Ln_CO2</b>				
G_αβ_G	9.30	−7.63	−70.96	0.1869
G_βO4_GS_ββ_GS	7.52	−9.28	−69.79	0.1512
GS_βO4_GS_ββ_GS	6.16	−9.67	−59.57	0.1238
G_βO4_G	6.16	−8.05	−49.59	0.1238
G_γβ_G	3.05	−7.50	−22.88	0.0613
G_βO4_GS_b5_G	2.71	−9.24	−25.04	0.0545
G_β5_G_γβ_GS	2.37	−9.32	−22.09	0.0476
G_βO4_G_β5_G	2.37	−8.85	−20.97	0.0476
<b>TOTAL</b>	<b>24.92</b>	<b>−69.54</b>	<b>−340.88</b>	<b>0.7968</b>
<b>Ln_India_depolymerized</b>				
G_γβ_G	4.97	−7.50	−37.28	0.1307
G_αβ_G	2.50	−7.63	−19.08	0.0658
G_βO4_GS	1.69	−7.58	−12.81	0.0444
GS_βO4_GS	1.55	−8.32	−12.90	0.0408
<b>TOTAL</b>	<b>10.71</b>	<b>−31.03</b>	<b>−82.06</b>	<b>0.2817</b>

Such high coefficients of correlation indicate that the energy of interaction that could be calculated for the oligomers for which theoretical interaction energy values are not known must present the same trend as those of the oligomers that constitute between 20% and 25% of the sample. These are the oligomers which were effectively used for the correlation between calculated and experimental results.

The coefficient of correlation is too low for the (Ln\_India) non-depolymerized, for the reasons given above. This is expected if one considers that this is the raw product obtained industrially. A more negative value of the theoretically calcu-

**Table 5.**

Calculated interaction energies of lignins with cellulose and experimental Young's modulus of lignins/cellulose composites

Designation	Dimers		Trimers	
	AutoDock (kcal/mol)	Young's modulus (MPa)	AutoDock (kcal/mol)	Young's modulus (MPa)
Ln_India	-47.01	0.2988	-134.68	0.6449
Ln_miscanthus	-155.06	0.6617	-22.09	0.0793
Ln_CO2	-143.42	0.3721	-197.46	0.4247
Ln_India_depolymerized	-82.06	0.2817	-	-

lated interaction energy means that the system of lignan and cellulose substrate is more stable and that the secondary forces attraction between lignan and substrate is stronger. Although from the interaction energy results in Table 5 and Fig. 8(a), (b) the trimers appear, in general, to be more strongly attracted to cellulose than dimers, this is not always the case (see Ln\_miscanthus, Table 5, Fig. 8(a), (b)). The molecular weight of the lignan thus does not appear to be the predominant factor in its interaction energy with the substrate. Higher molecular weight lignans such as trimers are sometimes linked more strongly to the substrate than lower molecular weight lignans such as dimers, and *vice versa*. Therefore, the important point is the ability of the oligomer to adapt itself to the surface of the substrate in such a manner that the interaction energy yields the strongest attraction of lignan and cellulose: this can happen for a dimer as well as for a trimer. This trend is evident for both theoretically calculated and for experimental results, as shown in Table 3 for the total interaction energy of lignan dimers and trimers with the cellulose substrate.

As the (Ln\_India\_depolym) has been depolymerised, it is exclusively composed of dimers. According to Fig. 5, the interaction energy with cellulose of (Ln\_India) and (Ln\_CO2) is determined mainly by trimers while for (Ln\_miscanthus) and (Ln\_India\_depol) lignins mainly by dimers.

#### 4. Conclusion

The low molecular weight lignins used are mostly composed of dimers and trimers. Lignins with high amounts of trimers appear to present a stronger interaction with the cellulose substrate. Due to the different compositions in oligomers of the four lignins it is difficult to make a comparison among them. Referring to Table 4, Ln\_India and Ln\_miscanthus had almost the same percentages of components and presented also similar interactions with the substrate both by molecular mechanics calculation as well as experimentally in terms of Young's modulus by TMA. Ln\_India showed highest interaction energy both by molecular mechanics calculation and experimental Young's modulus as a result of the highest proportion of trimers being present. The Ln\_India\_depolymerized lignin presented the lowest cal-

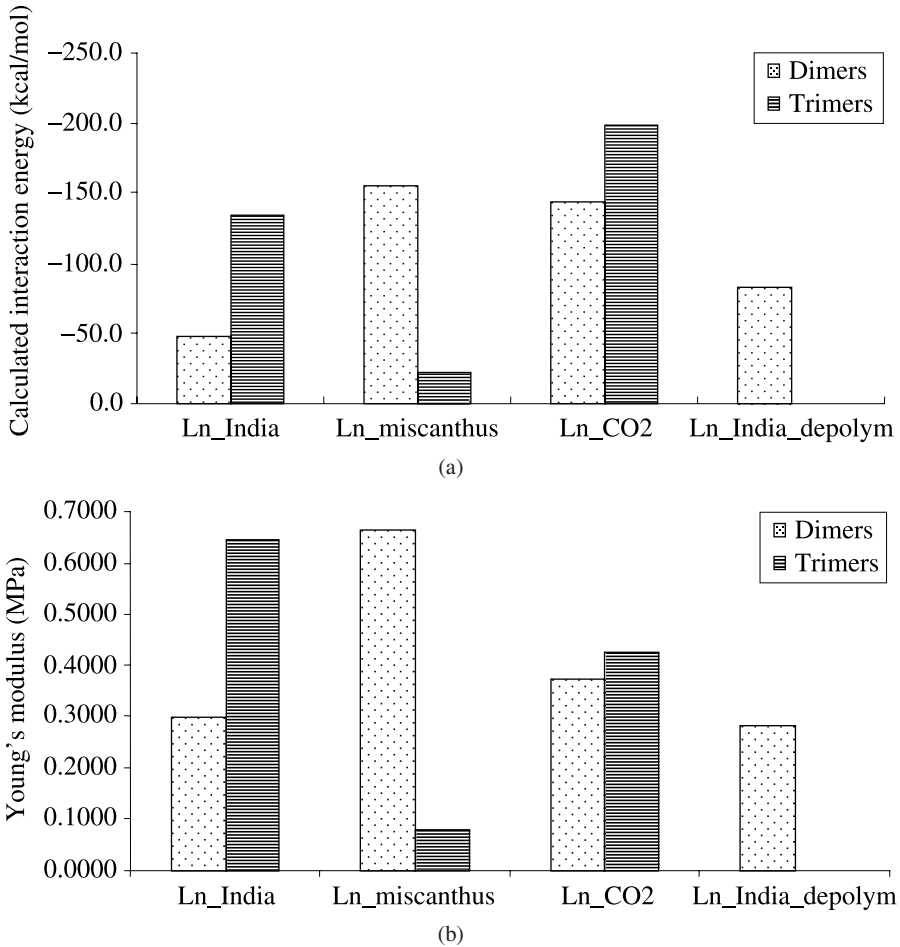


**Figure 8.** Strength of paper strip impregnated with 4 different types of lignins calculated on the basis of the trimers and dimers present from (a) molecular mechanics calculation, and (b) experimental thermomechanical analysis results.

culated interaction energy to which corresponded the lowest experimental value of Young's modulus too. This is expected as only 10% of the oligomers were used in the calculation and these were all dimers, hence, in general, yielding weaker interactions with the substrate. The conclusion appears to be that at least 20% of the oligomers need to be considered to expect some form of correlation between calculated and experimental results.

Ln\_CO<sub>2</sub> lignin presented a somewhat anomalous behaviour: it presented a stronger calculated attraction but the experimental Young's modulus value, although the second best of the four lignins tested, did not maintain the same expected trend and was lower than expected.

Usually trimers appear to present higher interaction energy than dimers although this depends on the type of linkage among their units. The molecular mechanics calculations indicated that a  $\beta$ -O-4-linked dimer has stronger attraction for the substrate than  $\beta\beta$  or  $\beta5$ -linked dimers. Consequently, the interaction energy is dictated by molecular weight and type of linkage within the lignan oligomers. Lignans with higher molecular weight in which the lignin units are linked by  $\beta$ -O-4 bonds [28] give interaction energy values indicating that the attraction between lignan and cellulose is stronger.

### Acknowledgements

The French author gratefully acknowledges the financial support of the CPER 2007-2013 “Structuration du Pôle de Compétitivité Fibres Grand’Est” (Competitiveness Fibre Cluster), through local (Conseil Général des Vosges), regional (Région Lorraine), national (DRRT and FNADT) and European (FEDER) funds.

### References

1. W. Boerjan, J. Ralph and M. Baucher, *Ann. Rev. Plant Biol.* **54**, 519–549 (2003).
2. T. Higuchi, in: *Biosynthesis and Biodegradation of Wood Components*, T. Higuchi (Ed.), pp. 141–160. Academic Press, Orlando, FL (1985).
3. E. Sjöström and A. Raimo, *Analytical Methods in Wood Chemistry, Pulping and Papermaking*. Springer, New York (1998).
4. A. Pizzi, *J. Adhesion Sci. Technol.* **20**, 829–846 (2006).
5. A. Pizzi, *Advanced Wood Adhesives Technology*. Marcel Dekker, New York (1994).
6. H. Nimz, in: *Wood Adhesives: Chemistry and Technology*, A. Pizzi (Ed.), Chapter 5. Marcel Dekker, New York (1983).
7. A. Pizzi and N. J. Eaton, *J. Adhesion Sci. Technol.* **1**, 191–200 (1987).
8. A. Pizzi, *J. Adhesion Sci. Technol.* **4**, 573–588 (1990).
9. A. Pizzi, *J. Adhesion Sci. Technol.* **4**, 589–595 (1990).
10. A. Pizzi and G. De Sousa, *Chem. Phys.* **164**, 203–216 (1992).
11. Granit<sup>®</sup> Lignin, Granit Recherche Développement SA, Lausanne, Switzerland.
12. R. El Hage, L. Chrusciel, N. Brosse, T. Pizzi, P. Navarrete, P. Sannigrahi and A. Ragauskas, in: *Proc. 2nd Nordic Wood Biorefinery Conference*, Helsinki, Finland, September 2–4, 2009.
13. S. Tapin-Lingua, unpublished results (2009).
14. N. Brosse, unpublished results (2009).
15. G. M. Morris, D. S. Goodsell, R. S. Halliday, R. Huey, W. E. Hart, R. K. Belew and A. Olson, *J. Comput. Chem.* **19**, 1639–1662 (1998).
16. D. A. Case, T. A. Darden, T. E. Cheatham, III, C. L. Simmerling, J. Wang, R. E. Duke, R. Luo, K. M. Merz, D. A. Pearlman, M. Crowley, R. C. Walker, W. Zhang, B. Wang, S. Hayik, A. Roitberg, G. Seabra, K. F. Wong, F. Paesani, X. Wu, S. Brozell, V. Tsui, H. Gohlke, L. Yang, C. Tan, J. Mongan, V. Hornak, G. Cui, P. Beroza, D. H. Mathews, C. Schafmeister, W. S. Ross and P. A. Kollman, AMBER 9 program, University of California, San Francisco (2006).
17. G. M. Morris, D. Goodsell, M. Pique, W. Lindstrom, R. Huey, S. Forly, W. Hart, S. Halliday, R. Belew and A. J. Olson, AutoDock Version 4.2. Automated Docking of Flexible Ligands to

Flexible Receptors. User Guide, Copyright © The Scripps Research Institute, La Jolla, CA, 1991–2009.

18. G. M. Morris, R. Huey, W. Lindstrom, M. F. Sanner, R. Belew, D. Goodsell and A. Olson, *J. Comput. Chem.* **28**, 1145–1152 (2009).
19. G. Schaftenaar and J. H. Noordik, *J. Comput.-Aided Mol. Design* **14**, 123–134 (2000).
20. L. Laaksonen, *J. Mol. Graph.* **10**, 33–34 (1992).
21. D. L. Bergman, L. Laaksonen and A. Laaksonen, *J. Mol. Graph.* **15**, 301–306 (1997).
22. P. Flükiger, H. P. Lüthi, S. Portmann and J. Weber, MOLEKEL 4.3 program, Swiss Center for Scientific Computing, Manno, Switzerland, 2000–2002.
23. S. Portmann and H. P. Lüthi, *Chimia* **54**, 766–769 (2000).
24. J. E. Lennard-Jones, *Proc. Roy. Soc. A* **106**, 463 (1924).
25. D. Frenkel and B. Smit, *Understanding Molecular Simulation*, 2nd edn. Academic Press, San Diego, CA (2002).
26. R. Huey, G. M. Morris, A. Olson and D. S. Goodsell, *J. Comput. Chem.* **28**, 1145–1152 (2007).
27. R. Huey, D. S. Goodsell, G. M. Morris and A. J. Olson, *Lett. Drug Design Discov.* **1**, 178 (2004).
28. D. Fengel and G. Wegener, *Wood: Chemistry, Ultrastructure, Reactions*, p. 613. Walter de Gruyter, Berlin (1984).
29. A. Pizzi, F. Probst and X. Deglise, *J. Adhesion Sci. Technol.* **11**, 573–590 (1997).
30. A. Pizzi, *J. Appl. Polym. Sci.* **63**, 603–617 (1997).

# Evaluation of Some Synthetic Oligolignols as Adhesives: A Molecular Docking Study

Carmen Martínez<sup>a</sup>, Miriam Sedano<sup>a</sup>, Abril Munro<sup>a</sup>, Pablo López<sup>a,\*</sup> and  
Antonio Pizzi<sup>b</sup>

<sup>a</sup> Facultad de Ingeniería en Tecnología de la Madera, Universidad Michoacana de San Nicolás de Hidalgo, Morelia, México

<sup>b</sup> ENSTIB-LERMAB, University of Nancy 1, B. P. 1041, F-88051 Epinal cedex, France

---

## Abstract

We have investigated alternative adhesives based on some oligomers that have structural units similar to lignins. The favorable interactions for a set of synthetic oligolignols were determined through a computational docking scheme, considering their conformational changes to adapt themselves on the surface of a three-dimensional model of cellulose I- $\beta$ , to describe and elucidate the interactions that drove their adhesion ability based on the minimum interaction energy calculated for each of the oligolignols conformations. The selected oligolignols included nine dimers, five trimers and one tetramer all of these were built from two lignin precursors, coniferol and sinapol, bonded in four different linkages:  $\beta$ -O4',  $\beta$ - $\beta'$ ,  $\beta$ -5' and  $\gamma$ - $\beta'$ . Our results showed that trimers were the most favorable oligolignols to dock over the cellulose model, considering their individual docking energy. We hope that this work contributes to the field of wood adhesives design and helps in understanding the interaction between the cellulose and structural components of lignin.

## Keywords

Lignin, adhesive, docking, lignin–cellulose interaction, molecular modeling

## 1. Introduction

Chemists and engineers have made several studies about the interaction between cellulose and lignin in the field of wood adhesives to improve their adhesion characteristics [1–5], all of these on an empirical basis [6, 7]. Considering the fact that lignin is the second major component of wood and its main biological function is as a cementing agent for wood cells [8], several studies have attempted to develop adhesives that reproduce or mimic these lignin properties [9, 10]. Furthermore, due to

---

\* To whom correspondence should be addressed. Facultad de Ingeniería en Tecnología de la Madera, Universidad Michoacana de San Nicolás de Hidalgo, Melon 398, Fracc. La Huerta, CP: 58080, Morelia, Michoacan, México. e-mail: plopez@umich.mx

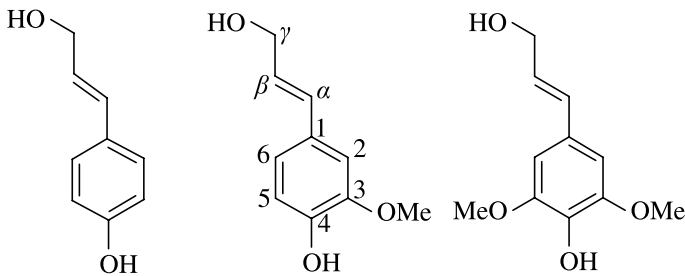


**Figure 1.** Lignin precursors: p-coumarol (left), coniferol (middle) and sinapol (right). Typical numbering is shown for the coniferol structure.

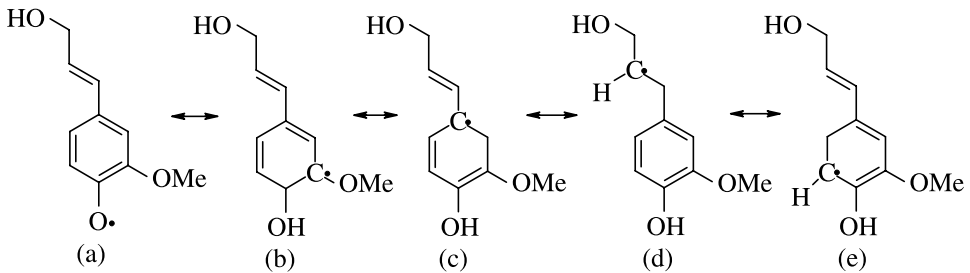


**Figure 2.** Free radical resonance structures of monolignols according to the resonance theory. Only coniferol is illustrated.

the fact that lignin occurs as a waste product in pulp processing in several countries (particularly in emerging economies) it becomes a very useful raw material.

Recently, adhesives that include lignin in their formulation have shown several properties similar to phenol-formaldehyde resins [11, 12] and are extensively utilized in the plywood, particleboard, fiberboard and laminated wood industries. The chemistry of the lignin-based adhesives has been studied from an empirical point of view [13]; however, the molecular mechanism and the interactions of the structural cross-linked 4-hydroxyphenylpropanoids of lignin that drive the adhesion phenomenon remain unclear.

Lignin structure is based on the assumption that it is derived from simple units of 4-hydroxyphenylpropane, and typically only three hydroxycinnamyl alcohols (p-coumarol, coniferol and sinapol) [14], these alcohols are named monolignols [15] and are shown in Fig. 1.

Lignin polymerization is initiated by an oxidative enzymatic dehydrogenation of monolignols [6], which form five different resonance structures [16] shown in Fig. 2. This leads to a large number of probable coupling reactions, yielding a disordered polymer.

The macromolecular structure of lignins could be produced by different combinations of interatomic linkages between two monolignols [17], but their relative abundance has not been established clearly [18]. The different lignin linkages are not clearly determined, because the structural complexity of lignin makes it difficult

to dissolve the whole polymer and thus hampers chemical and physical characterization [19]. Furthermore, inside wood fibers the coupling reactions between monolignol units are influenced by the environment of the cell wall [20], leading to a racemic polymer. Lignin is often called the “cementing agent” of wood cells [21], thus the characterization of its bonds is the first step to understand its cementing behavior.

Several attempts to obtain lignins *in vitro* have been made to synthesize oligolignols that reproduce some of the lignin linkages [22]; however, their exploitation in an adhesive formulation has not been reported. Moreover, in the computational chemistry framework some studies have explored the molecular interactions between monolignols or dilignols and polysaccharides surfaces [23]. Both procedures, experimental and computational, have provided some valuable insights into the nature of the interactions of lignin substructures and woody tissues; however, the complete set of the most abundant oligolignols in lignins has not been included in these studies.

The objective of the present computational chemistry study was to explore and to elucidate the most favorable interactions between a set of 15 oligolignols and a three-dimensional model of cellulose I- $\beta$ , evaluating their interaction energies in a molecular docking study. A set of synthetic oligolignols were selected to interact through a docking analysis with the cellulose model, because in this manner the most abundant linkages that occur in lignin are included.

## 2. Theoretical Background

In computational chemistry the procedure for predicting the interactions between a substrate and macromolecular targets in a molecular mechanics framework has been developed as *molecular docking scheme* [24]. Docking can be used to predict where and in which relative orientation a substrate binds to a macromolecule (also referred to as the binding mode or pose). This information may, in turn, be used to design more potent and selective analogs of the substrate [25]. Docking methods would find the global minimum in the interaction energy between the substrate and the target by exploring all available degrees of freedom for the substrate. Molecular docking is basically a conformational sampling procedure in which various docked conformations are explored to identify the most favorable substrate conformer that binds to a macromolecule. Rapid evaluation of the interaction energy between a substrate and a macromolecular target is achieved by precalculating atomic affinity potential for each atom type in the substrate [26]. In this procedure, the macromolecule is embedded in a three-dimensional grid and a probe atom is placed at each grid point. The interaction energy of this single atom with the macromolecule is assigned to a point inside the grid, yielding an affinity grid for each type of atom in the substrate, as well as a grid of electrostatic potential [27, 28]. Each point within the grid stores the potential energy of each atom type in the substrate that is due to all the atoms in the macromolecule. The energy of a particular substrate configuration

is then found by tri-linear interpolation of affinity values of the eight grid points surrounding each of the atoms in the substrate. Once the atomic affinity potential is precalculated, the docking simulation is carried out with the macromolecular target stationary throughout the simulation, i.e., its molecular geometry is frozen, and the substrate molecule performs a random walk in the space around the macromolecular target, applying a small random displacement to each degree of freedom of the substrate. These displacements result in a new macromolecule-substrate complex, whose energy is evaluated using the grid interpolation procedure described above. This new energy is compared to the energy of the previous step. If the new energy is lower, the new complex is immediately accepted. If the new energy is higher, the complex is accepted or rejected based on a Boltzmann distribution [29]. This search algorithm is known as Monte Carlo simulated annealing [30]. Simulated annealing allows an efficient exploration of the space of configurations generated by the macromolecule-substrate complexes, with multiple minima, which is typical of a docking problem. The separation of the calculation of the molecular affinity grids from the docking simulation provides modularity to the procedure, and allows exploring the molecular interactions in several substrate-macromolecule complexes, from constant dielectrics to finite difference methods and from standard 12-6 potential functions to distributions based on observed binding sites [31].

### 3. Lignin Precursors (Synthetic Oligolignols)

The selection of the synthetic oligolignols studied in this work was based on the fact that they reproduced many of the cross-linkages most frequent in lignins native structures [32]. The dominant moieties in lignins structures are the guaiacyl and the syringyl types. From a modeling perspective, we considered the major features of lignin to be aromatic rings, hydroxyl groups and methoxy groups and coniferol and sinapyl exhibit all of these features.

We use the following nomenclature to identify the oligolignol structure: CA for the guaiacyl moiety and SA for the syringyl moiety and for the combinations of interatomic linkages between two moieties the nomenclature was assigned according to the typical numbering of monolignols. Dilignols are displayed in Fig. 3, trilignols in Fig. 4 and a tetralignol in Fig. 5.

### 4. Three-Dimensional Model of Cellulose I- $\beta$

The model of a wood cell includes cellulose, hemicelluloses, metal ions, pectin analogues, lignin precursors and water; however inclusion of all of these components is computationally not feasible these days. Thus in order to delimit our study we have chosen the secondary wood cell wall, in which lignin and cellulose are dominant.

Cellulose is a homopolymer of  $\beta$ -(1-4) D-glucose molecules linked in a linear chain, with alternating sub-units in the crystalline structure being rotated through 180°. Native cellulose I microfibrils are highly ordered crystals and evidence from

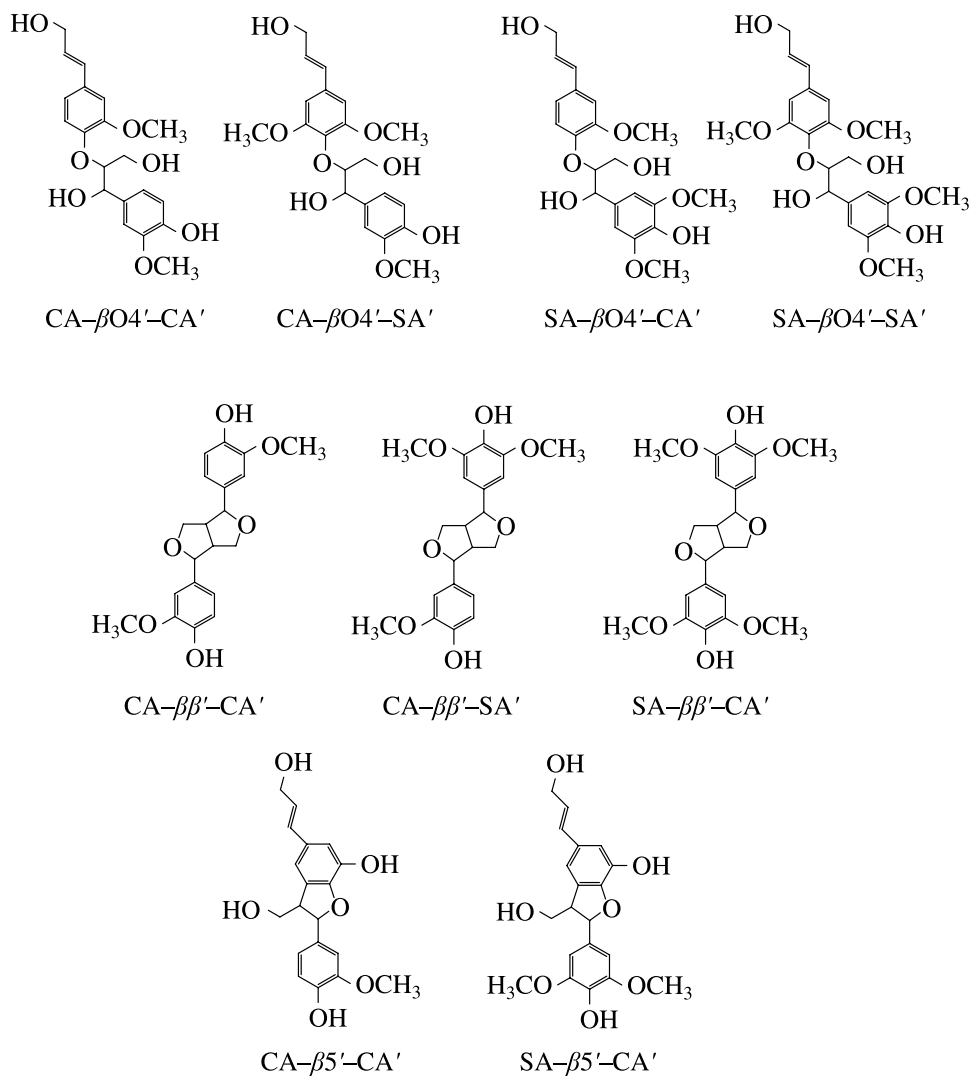


**Figure 3.** Dilignol structures used as the basis for studied synthetic oligolignols. The CA means guaiacyl moiety (coniferyl alcohol) and SA means syringyl moiety (sinapyl alcohol).

$^{13}\text{C}$ -NMR spectroscopy and electron diffraction suggests that these consist of both triclinic ( $I-\alpha$ ) and monoclinic ( $I-\beta$ ) crystalline forms [33–36]. Contrary to lignin, the macromolecular structure of cellulose is relatively well elucidated. Our study is limited to the  $I-\beta$  phase since it is reported to be dominant over the  $I-\alpha$  phase.

The three-dimensional model of cellulose  $I-\beta$  was built based on the crystal structure of native cellulose from X-ray measurements [37]. Our model has 12 D-glucose molecules along the cellulosic axle, 6 D-glucose molecules transverse to cellulosic axle and 3 superimposed lattices ( $6 \times 6 \times 3$  model) in a parallel arrangement and its unit cell is presented in Fig. 6.

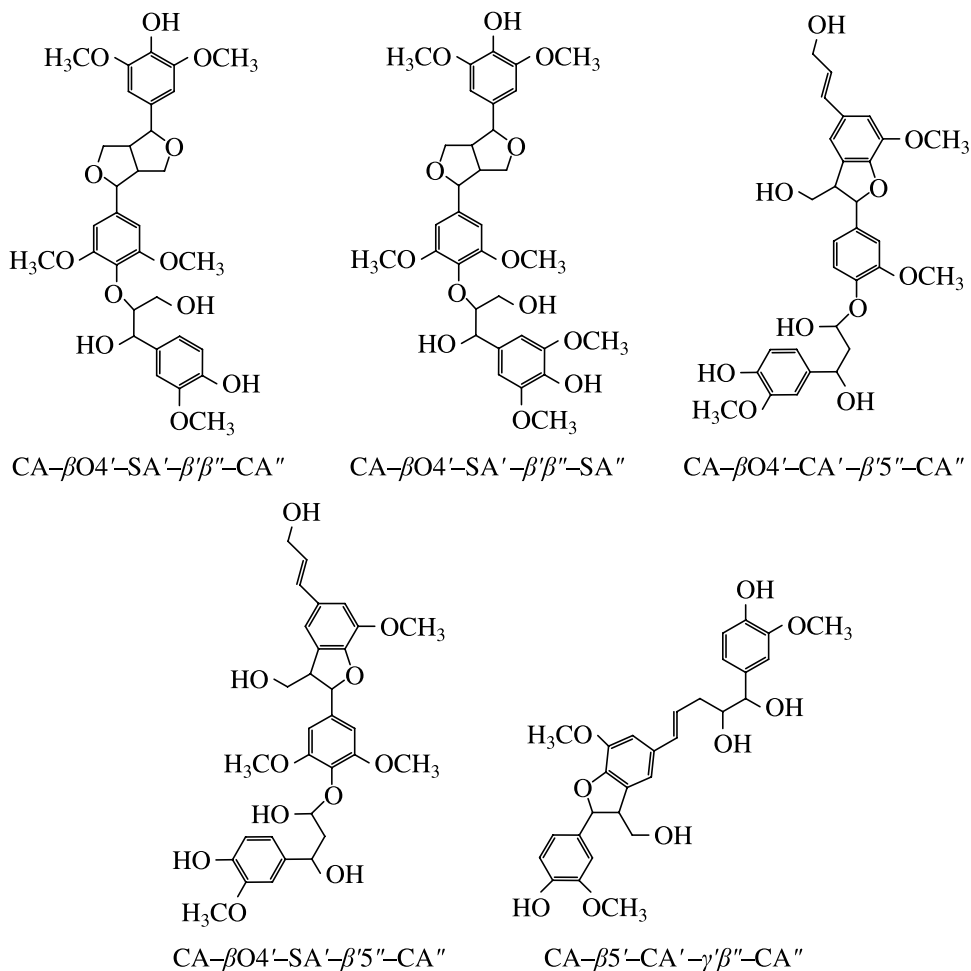


**Figure 4.** Trignol structures used as the basis for studied synthetic oligolignols. The CA means guaiacyl moiety (coniferyl alcohol) and SA means syringyl moiety (sinapyl alcohol).

This model contains enough information to simulate a crystallite of the cellulose I- $\beta$  native structure, which emulates the interaction in the docking process with the oligolignols.

## 5. Methodology

All molecular mechanics calculations were done using the program AutoDock, version 4.2.1. [38], which was developed to provide an automated procedure for predicting the interaction energy of substrates with macromolecular targets in a docking scheme. In our study, the ligands were the 15 synthetic oligolignols and the macromolecular target was the  $6 \times 6 \times 3$  model to simulate a cellulose I- $\beta$  crystallite described above. ChemBioOffice ultra, version 11.0.1, [39] was selected to

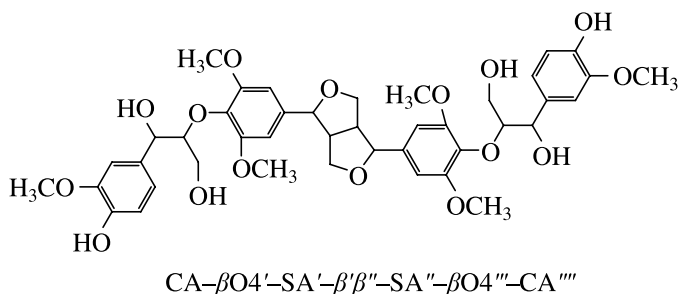


**Figure 5.** Tetralignol structure used as the basis for studied synthetic oligolignols. The CA means guaiacyl moiety (coniferyl alcohol) and SA means syringyl moiety (sinapyl alcohol).

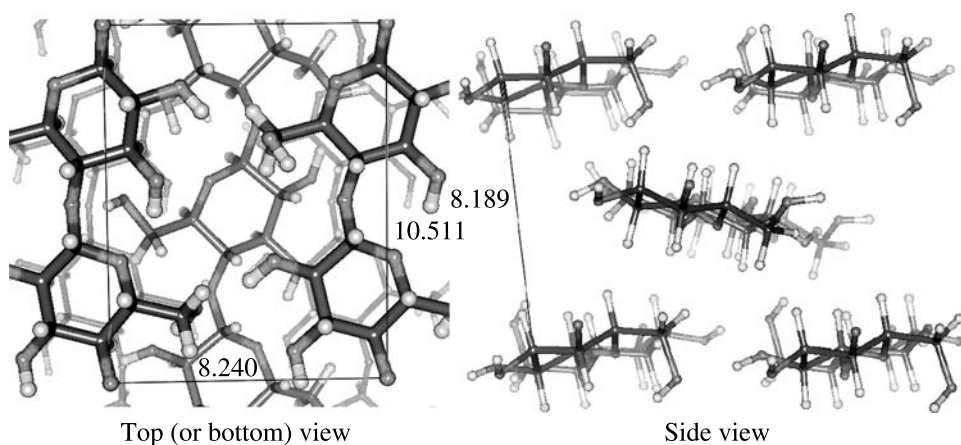


**Figure 6.** Schematic representation of the cellulose I-β model, units are in angstroms. The dimensions of the cellulose unit cell are displayed in two views: top (or bottom) view (left) show the distance along the cellulosic axle (10.511 Å) and the distance between cellulose chains at the same lattice (8.240 Å), meanwhile the side view displays the thickness of all three lattices (8.189 Å) of the cellulose unit cell.

sketch and build the molecular structures of the 15 oligolignols and the cellulose I-β three-dimensional model. Also the MGL-tools, version 1.5.4, [40] was utilized to set up, run and analyze AutoDock dockings and to visualize molecular structures.

The automated docking procedure for predicting the interaction energy was carried out independently for each oligolignol with the three-dimensional model of the cellulose I-β crystallite, and the initial configuration to start the docking calculations was built considering the substrates relatively far away from the macromolecule. We propose a three-dimensional arrangement similar to a plane (oligolignol) landing over an airstrip (macromolecule) as displayed in Fig. 7.

AutoDock provides several methods for doing the conformation search; however, the Lamarckian Genetic Algorithm (LGA) [41] provides the most efficient search for general applications and was our choice for the docking analysis. LGA begins with a population of random substrate conformations in random orientations and we

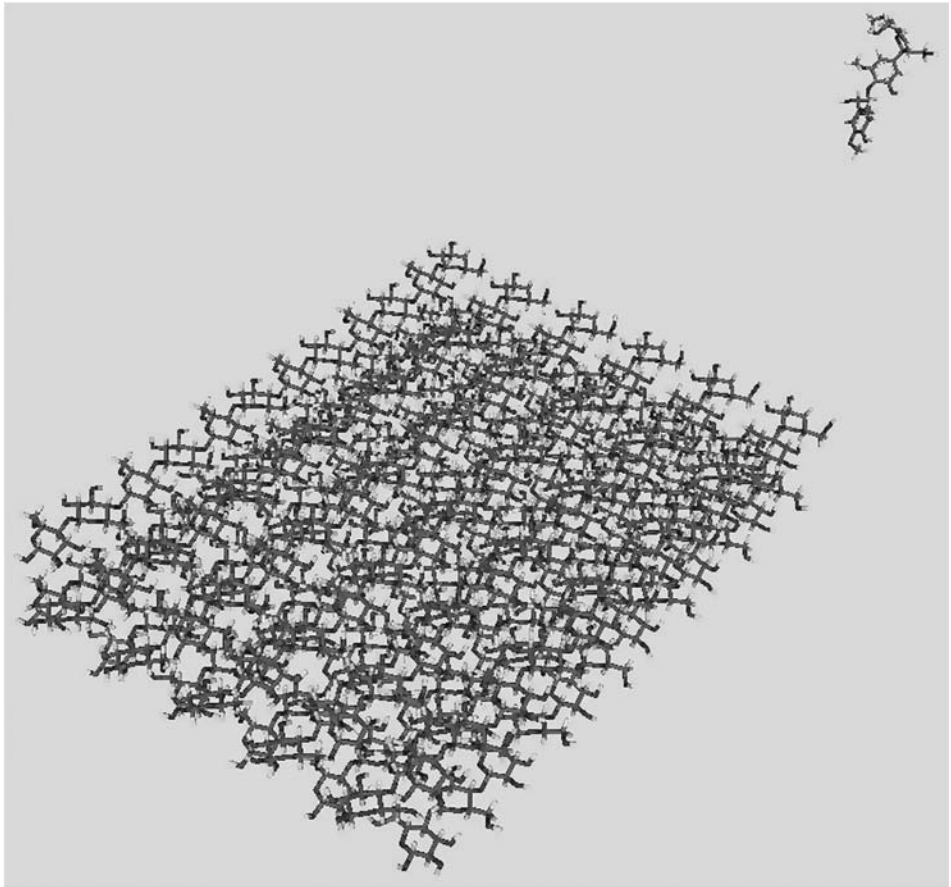


**Figure 7.** Model of the initial configuration to start the docking calculations built considering the oligolignols (substrates) relatively far away from the macromolecule cellulose I- $\beta$  crystallite (macromolecules). In our model, each oligolignol starts its docking as a plane landing on the cellulose I- $\beta$  crystallite (the airstrip).

found that setting up 50 orientations in the population of conformers covered the highest number of rotamers in all the oligolignols. The space where the oligolignols moved over the cellulose I- $\beta$  model was fixed considering the macromolecule to be inside and centered in a grid-box, whose dimensions were 126 grid-points in the long axis, 126 grid-points transversally to long axis and 90 grid-points in the layer axis, all with a spacing of 0.485 Å. Figure 8 displays the grid-box for the cellulose I- $\beta$  three-dimensional model.

The selected dimensions assumed that the hydroxyl groups at the edges of the cellulose I- $\beta$  did not generate any interaction with the oligolignols when docking process occurred, signifying that oligolignols interacted over only the surface of the three-dimensional model.

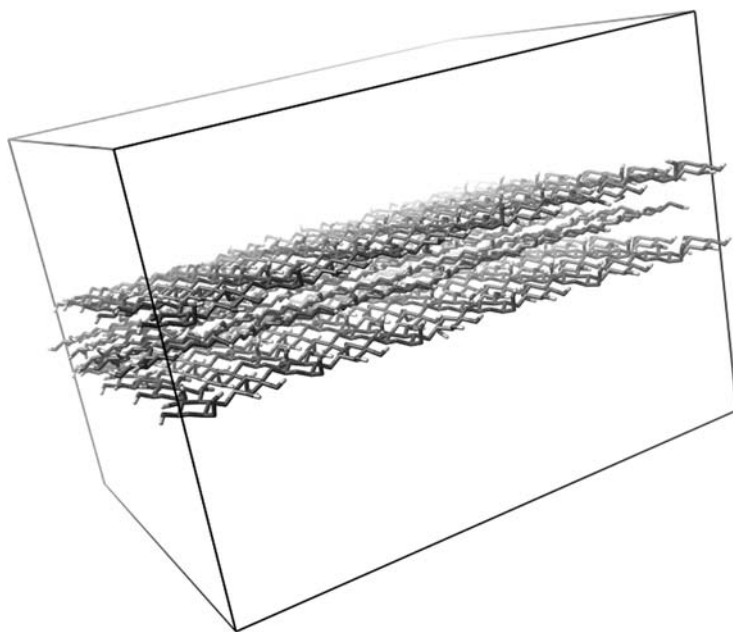


**Figure 8.** The grid-box surrounding the cellulose I- $\beta$  three-dimensional model, where the oligolignols moved in the docking simulation.

## 6. Results and Discussion

Study of chemical reactions is a simple matter, i.e., to determine whether a bond exists or not, since covalent bonds have rather fixed geometries. Adhesion begins with physical adsorption, but the process becomes complicated by ever-changing molecular geometries. Nevertheless, after a molecular mechanics calculation, we have the conformers of oligolignols in energetically favorable positions to interact with the cellulose I- $\beta$  macromolecular model.

The results of interaction energy and the number of H-bonds between each oligolignol and the cellulose I- $\beta$  macromolecular model are presented in Table 1.

The computational docking results indicate that the most favorable interaction was found when the tetralignol binds to the cellulose I- $\beta$  macromolecular model. In fact Table 1 has sorted the values for interaction energy from the most negative, i.e., the minimum, when the oligolignol–cellulose pair is very stable, to the least negative, i.e., the maximum which means poor stability of the oligolignol–cellulose pair. The first observation in the interaction energies is that the largest oligolignol presents the highest interaction energy, although the gap between the values for the trilignols and the dilignols was very close. Furthermore, the number of H-bonds was counted considering a binding distance less than 2.5 Å showing that the dilignols present similar results as trilignols and even as tetralignol.

The most favorable docked structures for the tetralignol, a trilignol and a dilignol are presented in Fig. 9, including the H-bonds formed.

**Table 1.**

Interaction energies obtained after the docking process in AutoDock, values are sorted from the minimum of interaction energy (most favorable interactions) to the maximum of interaction energy (least favorable interactions)

Oligolignols	Interaction (binding) energy in kcal/mol	Number of H-bonds
<i>Tetralignol</i>		
CA- $\beta$ O4-SA'- $\beta\beta$ -SA''- $\beta$ O4-CA'''	-10.21	3
<i>Trilignols</i>		
SA- $\beta$ O4-SA'- $\beta\beta$ -SA''	-9.67	6
CA- $\beta$ O4-SA'- $\beta\beta$ -SA''	-9.28	4
CA- $\beta$ O4-SA'- $\beta 5$ -CA''	-9.24	3
CA- $\beta 5$ -CA'- $\gamma\beta$ -CA''	-8.91	3
CA- $\beta$ O4-CA'- $\beta 5$ -CA''	-8.85	3
<i>Dilignols</i>		
SA- $\beta$ O4-CA'	-8.71	5
SA- $\beta$ O4-SA'	-8.32	4
CA- $\beta$ O4-CA'	-8.05	3
CA- $\beta\beta$ -SA'	-7.69	3
CA- $\beta$ O4-SA'	-7.58	3
SA- $\beta 5$ -CA'	-7.55	3
CA- $\beta 5$ -CA'	-7.10	3
CA- $\beta\beta$ -CA'	-7.08	3
SA- $\beta\beta$ -SA'	-5.70	2

Considering the fact that the adhesion phenomenon begins with physical interactions, it is necessary to consider that the coupling of oligolignols with the cellulose I- $\beta$  macromolecular model implies that favorable docked conformations and the H-bonds are generated. Observing Table 1 it appears that the longest oligolignol achieves the highest adhesion; however the interaction energy was obtained considering a single molecule of each oligolignol on the cellulose I- $\beta$  macromolecular model. Thus while tetralignol can achieve the minimum interaction energy, i.e., most favorable docking, the trilignols and the dilignols achieve more H-bonds. These results indicate that the number of dilignol or trilignol docked molecules on the cellulose I- $\beta$  macromolecular model can be higher than the tetralignol molecules.

An interesting observation for all the monolignols when they were docked on the cellulose I- $\beta$  macromolecular model was that all of these present their phenyl moiety almost parallel with the surface of the cellulose model. The tetralignol CA- $\beta$ O4-SA'- $\beta\beta$ -SA''- $\beta$ O4-CA''' docked conformer presents a diagonal coupling over the surface of the cellulose I- $\beta$  crystallite model. Although the tetralignol can be considered to be energetically favorable, its configuration over the cellulose I- $\beta$  crystallite model hampers the coupling of another tetralignol in its vicinity, yielding a poor adhesion interaction. From trilignols group in Table 1, the configuration SA- $\beta$ O4-SA'- $\beta\beta$ -SA'' was the most favorable docked structure, which was observed

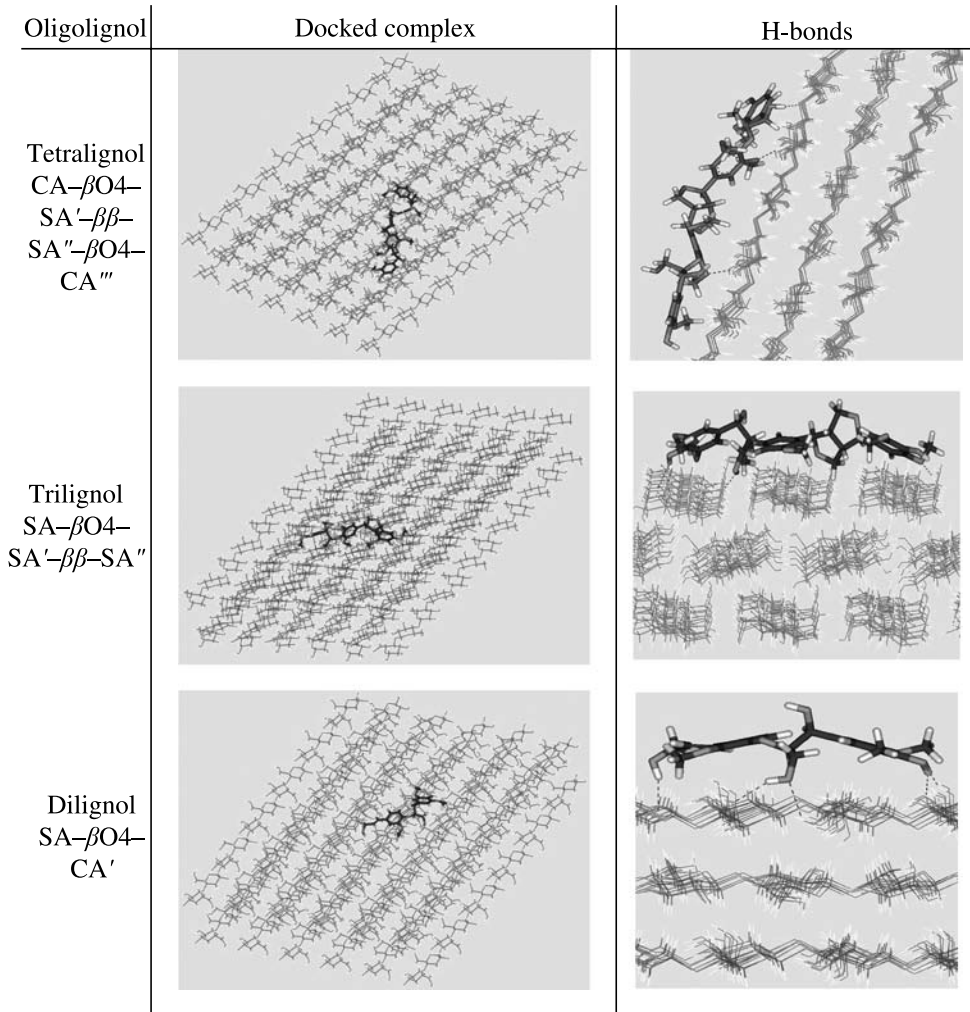


**Figure 9.** Most favorable docked conformations obtained for each synthetic oligolignol over the cellulose I- $\beta$  macromolecular model. The H-bonds are represented with blue dashed lines. Pictures in the first column display the oligolignol–cellulose complex after the docking calculation, whereas pictures in the second column display a close-up view of the H-bonds formed.

perpendicular to the cellulosic axle of the crystallite model. Its interaction energy was slightly lower than that of tetralignol (but trilignols permit that other similar molecules can dock or couple in their vicinity, yielding a set of trilignols that can maximize the adhesion interaction). The most favorable docked conformer of dilignols was the SA- $\beta$ O4-CA' which was observed parallel to the cellulosic axle of the crystallite model, thus it permits the maximum number of similar molecules to dock or couple over the cellulose I- $\beta$  crystallite model. Nevertheless, higher calculated interaction energy does not guarantee a good adhesion.

The hydroxymethyl groups in lignin precursors, the monolignols, appear to drive the adhesion phenomenon with the cellulose I- $\beta$  crystallite model, thus the syringyl moiety in the most favorable docked oligolignol promotes better interactions than the guaiacyl moiety. Furthermore, the  $\beta O4'$  and the  $\beta\beta'$  bonds are the linkages between monolignols that permit the favorable conformers to dock over the cellulose I- $\beta$  crystallite model.

## 7. Conclusions

The coupled conformations for a set of 15 synthetic oligolignols over a cellulose I- $\beta$  macromolecular model were studied and characterized. The interaction energy obtained for each oligolignol–cellulose pair provides insight into its adhesion ability. Although the longest oligolignol presented the minimum interaction energy, its size can hamper the docking of another tetralignol. The trilignols showed results that promote the adhesion interactions of the spatial kind as well as energetic ones. Furthermore these results show the importance of methoxy groups in the adhesion interactions. The methodology presented can be useful to describe the adhesive ability of synthetic oligolignols and thus can be a helpful tool in adhesives design.

## Acknowledgements

This work has been supported by a research grant from the National Science and Technology Council (CONACYT-México, Ciencia Básica 2006-57669), the Michoacan State Science and Technology Council (COECYT-Michoacan, 2007-2) and the Education Ministry (PROMEP-SEP).

The French author also gratefully acknowledges the financial support of the CPER 2007-2013 “Structuration du Pôle de Compétitivité Fibres Grand’Est” (Competitiveness Fibre Cluster), through local (Conseil Général des Vosges), regional (Région Lorraine), national (DDRT and FNADT) and European (FEDER) funds.

## References

1. H. Nimz, in: *Wood Adhesives Chemistry and Technology*, A. Pizzi (Ed.), chapter 5. Marcel Dekker, New York (1983).
2. A. Pizzi and N. J. Eaton, *J. Adhesion Sci. Technol.* **1**, 191–200 (1987).
3. A. Pizzi, *J. Adhesion Sci. Technol.* **4**, 573–588 (1990).
4. A. Pizzi, *J. Adhesion Sci. Technol.* **4**, 589–595 (1990).
5. A. Pizzi and G. de Sousa, *Chem. Phys.* **164**, 203–216 (1992).
6. A. Pizzi (Ed.), *Advanced Wood Adhesives Technology*. Marcel Dekker, New York (1994).
7. A. Pizzi and K. L. Mittal (Eds), *Handbook of Adhesive Technology*, 2nd edn. Marcel Dekker, New York (2003).
8. D. Fengel and G. Wegener, *Wood Chemistry, Ultrastructure, Reactions*, chapter 6, pp. 132–181. De Gruyter, Berlin (1989).

9. R. A. Young, M. Fujita and B. H. River, *Wood Sci. Technol.* **19**, 363–381 (1985).
10. N. E. El Mansouri, A. Pizzi and J. Salvado, *J. Appl. Polym. Sci.* **103**, 1690–1699 (2006).
11. M. A. Khana, S. Marghoob and V. P. Malhotra, *Int. J. Adhesion Adhesives* **24**, 485–493 (2004).
12. A. Pizzi, *J. Adhesion Sci. Technol.* **20**, 829–846 (2006).
13. A. Krzysik and A. R. Young, *Forest Products T.* **36**, 39–44 (1986).
14. T. Higuchi, in: *Biosynthesis and Biodegradation of Wood Components*, T. Higuchi (Ed.), pp. 141–160. Academic Press, Orlando, FL (1985).
15. K. Freudenberg, *Science* **148**, 595–600 (1965).
16. S. Barsberg, P. Matousek, M. Towrie, H. Jorgensen and C. Felby, *Biophys. J.* **90**, 2978–2986 (2006).
17. C. Martínez, J. L. Rivera, R. Herrera, J. L. Rico, N. Flores, J. G. Rutiaga and P. López, *J. Mol. Model.* **14**, 77–81 (2008).
18. R. S. Ward, *Chem. Soc. Rev.* **11**, 75–125 (1982).
19. E. Sjöstrom, *Wood Chemistry — Fundamentals and Application*, 2nd edn. Academic Press, San Diego, CA (1993).
20. C. Martínez, M. Sedano, J. Mendoza, R. Herrera, J. G. Rutiaga and P. Lopez, *J. Mol. Graph. Model.* **28**, 196–201 (2009).
21. A. Sakakibara and Y. Sano, in: *Wood and Cellulosic Chemistry*, D. N. S. Hon and N. Shirasi (Eds), chapter 4, pp. 109–174. CRC Press, Boca Raton, FL (2007).
22. J. Ralph and Y. Zhang, *Tetrahedron* **58**, 1349–1354 (1998).
23. C. J. Houtman and R. H. Atalla, *Plant Physiol.* **107**, 977–984 (1995).
24. W. L. Jorgensen, *Science* **254**, 954–955 (1991).
25. P. López-Albarran, Theoretical study of the drug-receptor interactions in the histamine H<sub>2</sub>-receptor, *PhD Thesis*, Departament of Chemistry, Universidad Autonoma Metropolitana, México (2005).
26. P. J. Goodford, *J. Med. Chem.* **28**, 849–857 (1985).
27. K. Sharp, R. Fine and B. Honig, *Science* **236**, 1460–1463 (1987).
28. S. A. Allison, R. J. Bacquet and J. McCammon, *Biopolymers* **27**, 251–269 (1988).
29. T. J. A. Ewing and I. D. Kuntz, *J. Comput. Chem.* **18**, 1175–1189 (1997).
30. D. Williamson and G. Jackson, *Mol. Phys.* **83**, 603–611 (1994).
31. B. Q. Wei, L. H. Weaver, A. M. Ferrari, B. W. Matthews and B. K. Shoichet, *J. Mol. Biol.* **337**, 1161–1182 (2004).
32. L. J. Landucci, *Wood. Chem. Technol.* **15**, 349–368 (1995).
33. R. H. Atalla and D. L. VanderHart, *Science* **223**, 283 (1984).
34. D. L. VanderHart and R. H. Atalla, *Macromolecules* **17**, 1465 (1984).
35. J. Sugiyama, T. Okano, H. Yamamoto and F. Horii, *Macromolecules* **23**, 3196 (1990).
36. J. Sugiyama, R. Vuong and H. Chanzy, *Macromolecules* **24**, 4168 (1991).
37. Y. Takabashi and H. Matsunaga, *Macromolecules* **24**, 3968 (1991).
38. R. Huey, G. M. Morris, A. J. Olson and D. S. A. Goodsell, *J. Comput. Chem.* **28**, 1145–1152 (2007).
39. CambridgeSoft, <http://www.cambridgesoft.com>
40. M. F. Sanner, *J. Mol. Graphics Mod.* **17**, 57–61 (1999).
41. G. M. Morris, D. S. Goodsell, R. S. Halliday, R. Huey, W. E. Hart, R. K. Belew and A. J. Olson, *J. Comput. Chem.* **19**, 1639–1662 (1998).

This page intentionally left blank

# Modification of Sugar Maple (*Acer saccharum*) and Black Spruce (*Picea mariana*) Wood Surfaces in a Dielectric Barrier Discharge (DBD) at Atmospheric Pressure

Frédéric Busnel<sup>a</sup>, Vincent Blanchard<sup>b,\*</sup>, Julien Prigent<sup>c</sup>, Luc Stafford<sup>c</sup>,  
Bernard Riedl<sup>a</sup>, Pierre Blanchet<sup>b</sup> and Andranik Sarkissian<sup>d</sup>

<sup>a</sup> Centre de Recherche sur le Bois, Faculté de Foresterie et de Géomatique, Université Laval, Québec (Québec) G1V 0A6, Canada

<sup>b</sup> FPInnovations–Division Forintek, 319 rue Franquet, Québec (Québec) G1P 4R4, Canada

<sup>c</sup> Département de Physique, Université de Montréal, Montréal (Québec) H3C 3J7, Canada

<sup>d</sup> Plasmionique, Montréal (Québec) J3X 1S2, Canada

---

## Abstract

This work examines the adhesion properties of sugar maple (*Acer saccharum*) and black spruce (*Picea mariana*) wood surfaces following their exposure to a dielectric barrier discharge at atmospheric pressure. Freshly sanded wood samples were treated in Ar, O<sub>2</sub>, N<sub>2</sub> and CO<sub>2</sub>-containing plasmas and then coated with a waterborne urethane/acrylate coating. In the case of black spruce wood, pull-off tests showed adhesion improvement up to 35% after exposure to a N<sub>2</sub>/O<sub>2</sub> (1:2) plasma for 1 s. For the same exposure time, adhesion improvements on sugar maple wood up to ~25% were obtained in Ar/O<sub>2</sub> (1:1) and CO<sub>2</sub>/N<sub>2</sub> (1:1) plasma mixtures. Analysis of the wettability with water contact angle measurements indicate that the experimental conditions leading to adhesion improvement are those producing more hydrophobic wood surfaces. In the case of sugar maple samples, X-ray photoelectron spectroscopy investigations of the near-surface chemical composition indicate an increase of the O/C ratio due to the formation of functional groups after exposure to oxygen-containing plasmas. It is believed that a combination of structural change (induced by UV radiation, metastable particles impingement, or both) and chemical change due to surface oxidation is responsible for the observed surface modification of black spruce and sugar maple wood samples.

## Keywords

DBD, wood, adhesion, atmospheric plasma, coating, urethane

## 1. Introduction

Over the last decades, wood industry has faced several challenges including economic crisis, emerging economies, and the appearance of substitution products. One

---

\* To whom correspondence should be addressed. E-mail: vincent.blanchard@fpinnovations.ca

major problem of wood products for some applications is their relatively short durability and the fast deterioration of their appearance. Several waterborne coatings have been developed to circumvent these limitations but these coatings are often characterized by poor adhesion to wood surfaces. The most common method to improve coating/wood adhesion is sanding. Freshly sanded wooden surfaces show distinctly higher work of adhesion between water and wood as compared to an aged wood surface [1]. This is because during aging, hydrophobic wood extractives migrate to the surface and, thus, decrease the surface energy [2]. Another approach to improve adhesion is the use of cold plasmas [3]. One particular advantage of such plasmas *versus* other alternatives such as heat treatment is their ability to uniformly modify the near-surface region without affecting the bulk properties [4]. Although low-temperature plasmas are already used in many technological fields such as microelectronics, packaging, biomaterials, decorative and functional coatings [5], it is a relatively recent technology for the wood industry.

In the case of common polymers such as polypropylene, polyethylene, polystyrene and poly(methyl methacrylate), many studies have shown that substantial changes in the chemical functionality, surface texture, wettability and bondability to other materials can be achieved by plasma treatment or ion irradiation [6–11]. Depending on the nature of the polymer being processed, several mechanisms have been invoked to explain the observed enhancement of the polymer properties *via* ion irradiation, including chain scission [12], cross-linking [13] and carbonization [14]. In the presence of chemical reactants, additional mechanisms need to be considered such as the adsorption or grafting of new reactive species, the elimination of weak boundary layers, the actual chemical changes such as oxidation, and the increase of surface roughness due to pitting [15].

While plasma-induced modification of synthetic polymers such as those listed above is well documented in the literature and, thus, relatively well understood, the results for wood surfaces are scarce and the level of knowledge remains at an embryonic state [16–19]. Podgorski and coworkers [20, 21] studied the influence of plasma and corona discharge treatments on fir species. They showed that wettability could be improved under specific conditions. Rehn *et al.* [22] showed that the fracture strength of glued black locust (*Robinia pseudoacacia*) increased and coating delamination reduced after exposure to a dielectric barrier discharge (DBD) in air. These results were attributed to the removal of the weak chemical and mechanical boundary layer on the wood surface. Lecoq *et al.* [23] exposed *Pinus pinaster* samples to a nitrogen DBD afterglow. This treatment made the wood surface either hydrophilic or hydrophobic depending on electrical parameters. These authors also observed an increase of the O/C ratio and the presence of carboxyl groups on the surface after exposure. Evans *et al.* [24] investigated the impact of a glow-discharge plasma derived from water on wettability and glue bond strength of four eucalyptus wood species. Blantocas *et al.* [25] showed that the fire and moisture resistance of different Philippine wood species was improved after treatment by low energy hydrogen ion showers. Recent studies also investigated plasma poly-